Frost flowers and sea-salt aerosols over seasonal sea-ice areas in north-western Greenland during winter–spring

Keiichiro Hara[1], Sumito Matoba[2], Motohiro Hirabayashi[3], and Tetsuhide Yamasaki[4]

[1] Department of Earth System Science, Faculty of Science, Fukuoka University, Japan
[2]Institute of Low Temperature Science, Hokkaido University, Japan
[3]National Institute of Polar Research, Tokyo, Japan
[4] Avangnaq, Osaka, Japan

Correspondence to: K. Hara (harakei@fukuoka-u.ac.jp)

Abstract. Sea-salts and halogens in aerosols, frost flowers and brine play an important role in atmospheric chemistry in polar regions. Simultaneous sampling and observations of frost flowers, brine, and aerosol particles were conducted around Siorapaluk in northwestern Greenland during December 2013 – March 2014. Results show that water-soluble frost flower and brine constituents were sea salt constituents (e.g., Na^+, Cl^-, Mg^{2+}, and Br^-). Concentration factors of sea-salt constituents of frost flowers and brine relative to seawater were 1.14–3.67. Sea-salt enrichment of Mg^{2+}, K^+, Ca^{2+}, and halogens (Cl^-, Br^-, and I) in frost flowers was associated with sea-salt fractionation by precipitation of mirabilite and hydrohalite. High aerosol number concentrations corresponded to occurrence of higher abundance of sea-salt particles in both coarse and fine modes, and blowing snow and strong winds. Aerosol number concentrations, particularly in coarse mode, were increased considerably by release from the sea-ice surface under strong wind conditions. Sulfate depletion by sea-salt fractionation was found to be slight in sea-salt aerosols because of heterogeneous SO_4^{2-} formation on sea-salt particles. However, coarse and fine sea-salt particles were found to be rich in Mg. Strong Mg enrichment might be more likely to proceed in fine sea-salt particles. Mg-rich sea-salt particles might be released from the surface of snow and slush layer (brine) on sea-ice and frost flowers. Mirabilite-like and ikaite-like particles were identified only in aerosol samples collected near new sea-ice areas. From the field evidence and results by previous works, we proposed sea-salt cycles in seasonal sea-ice areas.

1 Introduction

Frost flowers are ice crystals that contain brine and sea salts. They appear often during winter–spring in polar regions on the surfaces of new and young sea ice. Frost flowers play an important role as an interface among the atmosphere, sea ice, and ocean. Key conditions for formation and growth of frost flowers are (1) a cold atmosphere (below -15 °C) and (2) weak–calm winds (Perovich and Richter-Menge, 1994; Martin et al., 1995, 1996; Style and Worster, 2009; Roscoe et al., 2011). Vertical gradients of temperature and relative humidity near the sea-ice surface are crucially important for the appearance of frost flowers. Frost flowers can be formed by condensation of water vapour on nodules on new and young sea ice. Results of earlier studies (e.g., Domine et al., 2005; Douglas et al., 2012) show that water vapor is initially supplied to the atmosphere, with sublimation and/or evaporation occurring from the warm sea-ice surface. Strong vertical gradients of air temperature above the sea-ice surface engender supersaturation of water vapor near the sea-ice surface; then the gradients induce condensation of water vapor (i.e., frost flower formation). The concentrated seawater (i.e. brine) is present on new and young sea ice. Consequently, brine with high salinity migrates upwardly and gradually on frost flowers (Perovich and Richter-Menge, 1994; Martin et al., 1996; Roscoe et al., 2011). Under cold conditions, solutes with lower solubility in brine can be precipitated in and on sea ice and frost flowers depending on the temperature. Previous investigations (e.g., Marion, 1999; Koop et al., 2000; Diekmann et al., 2008, 2010; Geilfus et al., 2013) have revealed that several salts can be precipitated at -2.2 °C (ikaite, $CaCO_3 \bullet 2H_2O$), -8.2 °C (mirabilite, $Na_2SO_4 \bullet 10H_2O$), -15 °C (gypsum, $CaSO_4$), -22.9 °C (hydrohalite, $NaCl \bullet 2H_2O$), -28°C

($NaBr•5H_2O$), -33 °C (sylvite, KCl), -36°C ($MgCl_2•12H_2O$), and -53.8 °C (antarcticite, $CaCl_2•6H_2O$). The salt precipitation at lower temperatures causes changes to sea-salt ratios in brine and frost flowers, known as *sea-salt fractionation*.

Frost flowers have a fine structure. Earlier field and laboratory experiments indicated frost flowers as less fragile, even under strong winds, in spite of their fine structure (Obbard et al., 2009; Roscoe et al., 2010). In addition, results of model studies have implied that blowing snow contributes importantly to atmospheric halogen chemistry (Yang et al., 2010; Abbatt et al., 2012; Lieb-Lappen and Obbard, 2015). Because of the lower number density of aerosol particles in polar regions, especially in Antarctic regions, emission of sea-salt particles from sea-ice areas is an important aerosol source during winter–spring (e.g., Wagenbach et al., 1998; Rankin et al., 2000; Hara et al., 2004, 2011, 2012, 2013). Actually, sea-salt particles released from sea-ice areas are dispersed from the boundary layer to the free troposphere (up to ca. 4 km) over Syowa Station, Antarctica through vertical motion by cyclone activity (Hara et al., 2014), and into the interior (Dome F Station and Concordia Station) of the Antarctic continent (Hara et al., 2004; Udisti et al., 2012). Vertical transport of the sea-salt particles originating from sea ice can act as a supply of cloud condensation nuclei (CCN) and ice nuclei (IN) in the upper boundary layer – free troposphere. Because of the horizontal transport of sea-salt particles into the Antarctic plateau, the Na^+ records in ice cores taken in the inland area have been used recently as a proxy of the sea-ice extent (e.g., Wolff et al., 2003, 2006).

As described above, sea-salt fractionation proceeds on new and young sea ice. For that reason, sea-salt ratios in sea-salt particles (or aerosols) released from sea-ice areas differ from those of the bulk seawater ratio (Hara et al., 2012, 2013). For instance, Mg-rich sea-salt particles and aerosol particles containing $MgCl_2$ and $MgSO_4$ were identified to a remarkable degree at Syowa Station during winter–spring because precipitation of mirabilite and hydrohalite engenders Mg-enrichment in sea-salt particles (Hara et al., 2012, 2013). Because the relative humidity of Mg-salt deliquescence, such as that of $MgCl_2$, is lower than that of NaCl (e.g., Kelly and Wexler, 2005), sea-salt fractionation can engender modification of aerosol hygroscopicity, which is closely related to phase transformation, heterogeneous reactions, and abilities of cloud condensation nuclei and ice nuclei. In addition to sea-salt fractionation, sea-salt ratios in frost flowers and aerosols can be altered gradually by heterogeneous reactions in a process known as *sea-salt modification*. Furthermore, frost flowers have large specific surface area: 63–299 $cm^2\ g^{-1}$ (mean, 162 $cm^2\ g^{-1}$) at Hudson Bay, Canada (Obbard et al., 2009) and 185 (+80, -50) $cm^2\ g^{-1}$ at Barrow, Alaska (Domine et al., 2005). For that reason, larger surface area, earlier studies have assessed the potential of frost flowers as reaction sites (e.g., Kaleschke et al., 2004, references in Abbatt et al., 2012). Sea-salt modification in sea-salt aerosols, and sea salts in and on frost flowers and sea ice can act as potential sources of gaseous reactive species. For instance, gaseous reactive halogen species (e.g., Br_2, HOBr, Br, and BrO) induce depletion of ozone and mercury near the surface in both polar regions during the polar sunrise (Barrie et al., 1988; Schroeder et al., 1998; Foster et al., 2001; Ebinghaus et al., 2002). According to laboratory experiments conducted by Koop et al. (2000), Br^- can be enriched in frost flowers by sea-salt fractionation. Reportedly, Br^- enrichment occurs slightly in frost flowers in the Weddell Sea, Antarctica (Rankin et al., 2002). Slight Br^- enrichment to Na^+ has also been observed in a few samples collected at Barrow, Alaska, although there was no Br^- enrichment in same samples of frost flowers and brine (Douglas et al., 2012). Additionally, results of some earlier results of studies have shown non-significant Br^- enrichment in frost flowers at Barrow and Hudson Bay (Alvarez-Aviles et al., 2008; Obbard et al., 2009). Therefore, many issues persist with respect to sea-salt and halogen chemistry of aerosols and frost flowers. They demand further measurement and discussion.

To elucidate the atmospheric impact of fractionated sea-salt particles and their relation between sea-salt particles in the atmosphere and frost flowers on sea ice, one must ascertain their (1) chemical properties (e.g., concentrations, ratios, and pH) of frost flowers and brine, and (2) the physical and chemical properties of aerosols (e.g., size distribution, constituents, and

mixing states) above seasonal sea ice with frost flowers. Despite the importance, simultaneous observations and measurements of aerosols and frost flowers over seasonal ice areas with frost flower appearance have not been reported for polar regions, although sampling and observations of frost flowers have been conducted in the Arctic (e.g., Alvaraz-Aviles et al., 2008; Douglas et al., 2012) and Antarctica (Rankin et al., 2000, 2002). This study aims to understand sea-salt cycles in the seasonal sea-ice areas such as sea-salt fractionation on sea-ice surface including frost flowers, brine and snow, its aging processes, and release of the fractionated sea-salt particles to the atmosphere from simultaneous measurements and sampling of aerosols, frost flowers, and brine around northwestern Greenland during winter–spring.

2 Samples and Analysis

2.1 Sampling sites and conditions

Figure 1 shows simultaneous observations of frost flowers, brine, seawater, and aerosols conducted on new and young sea-ice area in Robertson fjord near Siorapaluk in northwestern Greenland from mid-December, 2013 through mid-March, 2014. In the fjord, the open sea surface appears during summer. Sea ice formed gradually from October, 2013. Sea ice flowed out several times from the fjord by the action of sea tides, heaving, and strong winds (Fig. 1) before and during the measurements taken for this study. Therefore, sea ice of different ages (new – very old) was present in the fjord in front of Siorapaluk. We chose Sites I–III (new – young sea ice; less than 1 cm – ca. 35 cm thickness) as sampling sites of aerosols, frost flowers, brine, and seawater. Site I was approximately 2 km distant from Siorapaluk. The sea ice on Site I had flowed during 10–12 February, 2014 (shown as a red broken line); then it refroze. Site II had younger sea ice than Site I did. Before several days to a week prior, an open-lead appeared around Site II. Thereafter, new sea ice was formed. The refrozen lead width was 2–6 m. Site IIIa and IIIb were close to the sea-ice edge. The sea surface appeared off Siorapaluk on approximately 1 March by sea-ice breakage and strong winds (shown by the blue broken line). Then, new sea ice formed again. The new sea ice at Site IIIa and IIIb (less than 1 cm thickness) was a few days old. On 3 and 5 March, we traversed along the new sea-ice area (blue broken line in Fig.1) to observe the sea-ice conditions and appearance of frost flowers on the sea-ice. Then, we chose sampling sites (IIIa and IIIb) where was safely accessible. New sea ice formed gradually on the sea surface at Site IIIa and IIIb (photographs, Fig. 1). We accessed sampling sites with frost flowers on foot and by dog sledge from Siorapaluk. Sampling sites are presented in Fig. 1.

2.2 Sampling of frost flowers, brine, snow, and seawater

Sampling of frost flowers, brine (slush), and seawater was conducted from 20 February, 2014 through 3 March, 2014 on sea ice near Siorapaluk. Frost flowers were taken from the sea-ice surface using a clean stainless steel shovel. During the campaign, snowfall and blowing snow occurred occasionally. On the frost flower and slush layer at site I and II, snow was slightly present to the extent to that the fine structure of frost flowers was identified clearly. All bodies of the frost flowers above sea-ice surface were collected if the forms of frost flowers were matured and dry. The frost flowers were collected with the coating brine water if the form of frost flowers was young and coated with brine water. When snow was present on the frost flower and slush layer, some frost flower samples can contain slightly snowy pieces because of the difficulty of segregation. Brine samples were collected by shaving off a thin layer of the sea-ice surface and coating the brine water in proximity to the frost flowers. With the exception of new sea-ice at Site III with thickness of a few centimeters, slush was sampled on sea-ice where frost flowers were formed. It was difficult to collect only brine from the slush layer. Therefore, the slush layer was sampled as "brine samples" in this study. Brine (slush) samples contained not only brine but also ice and snow, although brine was considerably dominant in sea-salt concentrations. Snow on sea-ice was also taken using a clean stainless steel shovel from the location with snow accumulation (< 3 cm depth) without frost flowers at Sites I and II. Pieces of frost flowers, brine (slush) samples, and snow were moved into each polyethylene bag (Whirl-pak; Nasco). Using a dropper, seawater samples were collected in polypropylene bottles from a crack in the sea ice or a hole we made in the sea ice. All samples were melted at ambient temperature. The H^+ concentration (i.e., pH) of the liquid sample was measured using a portable pH meter (B-212;

Horiba Instruments Ltd.). Then residue of the sample was transferred to polypropylene bottles. The samples in the bottles were kept in colder conditions below - 20°C in Greenland. Then, samples were unfrozen during transport (ca. 3 days) to our laboratory in Japan because of the difficulty of carrying frozen samples in an airplane. After the bottled liquid samples were transported to Japan, all were kept frozen in a cold room until chemical analyses were conducted.

2.3 Aerosol sampling and measurements

Aerosol measurements and direct sampling were conducted over seasonal sea ice around Siorapaluk, Greenland from 17 December, 2013 through 7 March, 2014. Aerosol number concentrations were measured using a portable optical particle counter (OPC, KR12A; Rion Co. Ltd.). The measurable size range was D_p >0.3, >0.5, >0.7, >1.0, >2.0, and >5.0 μm. The OPC packed in an insulator box was set at ca. 1 m above the sea-ice surface by a tripod. Aerosol number concentrations were recorded every 23–25 s, corresponding to 1 L air sucking, during aerosol direct sampling. Details of OPC measurements were described in Hara et al. (2014).

Direct aerosol sampling was made using a two-stage aerosol impactor. Carbon-coated collodion thin films supported by a Ni micro-grid (square-300 mesh; Veco Co.) were used as sample substrates in this study. The cut-off diameters (aerodynamic diameter) of the impactor were 2.0 and 0.2 μm at a flow rate of ca. 1.2 L min^{-1}. The impactor was set at ca. 1 m above the seasonal sea-ice surface, similarly to OPC measurement. Direct aerosol sampling was conducted for 10-15 min depending on the aerosol number concentrations. Aerosol samples were kept in polyethylene capsules immediately after aerosol measurements and sampling. The polyethylene capsules with aerosol samples were packed into polyethylene zipper bags. All bags with aerosol samples were put into an airtight box together with a desiccant (Nisso-Dry M; Nisso Fine Co., Ltd.) until analysis at room temperature to prevent humidification that can engender morphology change and efficient chemical reactions, as described by Hara et al. (2002, 2005, 2013, 2014). All aerosol samples presented in this study were analyzed and observed within one year after sampling.

Meteorological data (air temperature, relative humidity, air pressure, wind direction, and wind speed) were measured using an auto-weather station (HOBO U30-NRC Weather Station; Onset Computer Corp.), which was set on the coast near Siorapaluk and ca. 1 km away from the village. Meteorological data were recorded to the data logger of the auto-weather station with a time resolution of 5 min. A thermorecorder (TR-7Wf; T and D Corp.) and thermosensor (TR1106; T and D Corp.) were used for measurements of temperature of seawater, slush layer (brine) on sea ice, base of frost flowers on slush layer, and the atmosphere above the top of the frost flowers.

2.4 Sample analysis

2.4.1 Analysis of frost flower, brine, snow, and seawater

Re-frozen samples of frost flower, brine, snow, and seawater were melted in ambient temperature before chemical analyses. Concentrations of ion species (Na^+, K^+, Mg^{2+}, Ca^{2+}, Cl^-, NO_3^- and SO_4^{2-}) in frost flowers, brine and seawater were measured using ion chromatography (ICS 2100; Thermo Fisher Scientific Inc.) after 10^3-fold dilution by ultrapure water, whereas those in snow were determined without dilution. A guard column (IonPac CG12; Thermo Fisher Scientific Inc.), column (IonPac CS12; Thermo Fisher Scientific Inc.) and a 20 mM CH_3SO_3H eluent for the cation measurement, and Guard column (IonPac AG14; Thermo Fisher Scientific), column (IonPac AS14; Thermo Fisher Scientific Inc.) and 3.5 mM NaOH eluent were used for the anion measurement. Concentrations of Br^- in frost flower and brine were measured using an ion chromatograph-mass spectrometer (IC-MS) after 10^6-fold dilution using ultra-pure water. Ionic contents in samples were separated using ion chromatography with a guard column (IonPac AG11-HC; Thermo Fisher Scientific Inc.), a column (IonPac AS11-HC; Thermo Fisher Scientific Inc.) and gradient KOH eluent (4–36 mM), and were injected into a mass spectrometer (6100 series single

quadrupole LC/MS; Agilent Technologies Inc.). The detection limit of Br^- in IC-MS was 0.9 ng L^{-1}. Iodine concentrations in frost flower and brine were measured after 10^3-fold dilution using ultra-pure water using an inductively coupled plasma-mass spectrometer (ICP-MS, 7700 series single quadrupole ICP-MS; Agilent Technologies Inc.). The RF power and flow of carrier Ar gas were, respectively, 1550 W and 0.80 L min^{-1} in ICP-MS analysis. The detection limit of iodine used for this study was 17 ng L^{-1}. Samples of frost flowers and brine were injected into ICP-MS after melting. Therefore, iodide and iodate were not divided in this study. Details of IC-MS analytical procedures are described elsewhere by Hirabayashi et al. (preparation for publication). We calculated concentration factors (CF-X) with concentrations of chemical species (X) in samples divided by concentration of X in seawater to evaluate the concentration processes of the chemical species during the formation and aging of frost flowers. Analytical errors in each analytical method were estimated from reproducibility of determination of standard solutions with the concentrations with similar to the field samples.

2.4.2 Analysis of individual aerosol particles

Individual aerosol particles on the sample substrate were observed and analyzed for this study using a scanning electron microscope equipped with an energy dispersive X ray spectrometer (SEM-EDX, Quanta FEG-200F, FEI, XL30; EDAX Inc.). The analytical conditions were 20 kV accelerating voltage and 30 s counting time. Details of analytical procedures were in accordance with Hara et al. (2013, 2014). We analyzed 1261 particles in coarse mode (mean, 41 particles per sample) and 6337 particles in fine mode (mean, 192 particles per sample). Most aerosol-sampled areas on the substrates in this study were analyzed in coarse mode in this study. Although we attempted to analyze as many coarse particles as possible, the lower aerosol number concentrations in coarse mode limit the number of the aerosol particles analyzed in this study.

3. Results

3.1 Meteorological conditions during the campaign

Figure 2 depicts time variations of air temperature, relative humidity, and wind speed during our measurement. The air temperature was -34.2 – +1.8 °C. Colder conditions below -20°C occurred on the day of year (DOY) = 47.5–58.6 (February 17–28, 2014) during our intensive sampling and observations of aerosols and frost flowers. Because of an approaching cyclone, several strong wind events occurred during the campaign. Particularly strong winds in DOY = 39.7–41.2 (9–11 February) caused breaks and outflows of sea ice from the front of Siorapaluk (ca. 1 km away). Then the seawater started refreezing immediately after recovery of the weather. Sea ice off Siorapaluk (ca. 5–6 km away) broke and flowed out again off Siorapaluk by storm conditions on DOY = 58.9–60.3 (February 28 – March 1). Sea ice formed after the recovery of weather conditions. Frost flowers appeared on the new sea ice in both cases.

3.2 Conditions of frost flowers and sea-ice

Sea ice conditions where frost flowers formed can be categorized as three types in this study: young ice (Site I), younger ice in refrozen leads between young ice (Site II), and new sea ice (Site IIIa and IIIb). Figure 3 depicts photographs of frost flowers observed at Site I, categorized as young ice (Fig. 3a) on 20 February. The sea-ice surface was partly covered with thin snow. Frost flowers were formed patchily on the ice surface without snow cover. The sea-ice surface underneath frost flowers was wetted by brine (sherbet-like). Figure 3b presents a close up photograph of frost flowers observed on 22 February at the same site as that observed on 20 February. Salt crystals deposited on the branches of frost flower crystals were identified. Frost flowers at Site I were covered completely with snow after the storm on 28 February – 1 March. Figure 3c shows frost flowers observed at Site II (Fig. 1). The sea-ice surface underneath frost flowers was wet by brine. Figure 3d shows frost flowers observed at Site IIIa (Fig. 1) on 4 March. The site was at the edge of sea ice, close to open water. The frost flower diameter was approximately 5 mm. The sea-ice surface was covered with brine water (Fig. 3e). The frost flower crystals were partially

submerged in the brine water. During our campaign (December, 2013 – March, 2014), frost flowers were absent on old and very old sea-ice. Although snow covered dry surface of old and very old sea-ice patchily before the storm, bare sea-ice was apparent after the storm (Fig. 3f).

3.3 Concentrations of sea salts in frost flowers, brine, and snow on sea ice

Figure 4 depicts relations among the respective constituents of frost flowers, brine, snow, and seawater found in this study. Logarithmic plots of Fig.4 were shown in Figure S1. Concentrations of Na^+ in frost flowers and brine were 48–154 mmol L^{-1}, which greatly exceeded the seawater concentration. The concentration factors of Na^+ (CF_{Na}) in frost flowers and brine were 1.14–3.67, which roughly approximated values reported by previous studies (e.g., Rankin et al., 2002; Alvarez-Aviles et al., 2008). By contrast, the Na^+ concentrations in snow samples collected on sea-ice were 1 – 2 orders lower than that of seawater. The Na^+ concentrations of fresh snow on sea-ice were lower than 0.1 mmol L^{-1}. Actually, Na^+ concentration were 0.4 – 3.2 mmol L^{-1} in the aged snow on sea-ice. High correlation among constituents was identified in frost flowers, brine, and snow, as follows.

Frost flowers:

$[Cl^-] = 1.302\ [Na^+] + 2.158$ (R^2 =0.969)

$[Br^-] = 0.0022\ [Na^+] + 0.025$ (R^2 =0.910)

$[I] = 1.17 \times 10^{-6}\ [Na^+] + 5.867 \times 10^{-4}$ (R^2 =0.791)

$[Mg^{2+}] = 0.122\ [Na^+] – 0.761$ (R^2 =0.982)

$[K^+] = 0.023\ [Na^+] – 0.063$ (R^2 =0.988)

$[Ca^{2+}] = 0.023\ [Na^+] – 0.019$ (R^2 =0.996)

Brine:

$[Cl^-] = 1.421\ [Na^+] – 21.35$ (R^2 =0.964)

$[Br^-] = 0.0020\ [Na^+] + 0.06$ (R^2 =0.962)

$[I] = 1.10 \times 10^{-6}\ [Na^+] + 3.25 \times 10^{-5}$ (R^2 =0.842)

$[Mg^{2+}] = 0.114\ [Na^+] – 0.8267$ (R^2 =0.982)

$[K^+] = 0.022\ [Na^+] – 0.140$ (R^2 =0.988)

$[Ca^{2+}] = 0.021\ [Na^+] – 0.023$ (R^2 =0.972)

Snow:

$[Cl^-] = 1.315\ [Na^+] + 0.02$ (R^2 =0.972)

$[Mg^{2+}] = 0.035\ [Na^+] + 0.02$ (R^2 =0.751)

$[K^+] = 0.024\ [Na^+] – 0.002$ (R^2 =0.997)

$[Ca^{2+}] = 0.026\ [Na^+] + 2\times10^{-5}$ (R^2 =0.994)

This study did not determine the Br^- and I concentrations in the snow samples. High determination coefficients imply strongly that the constituents are sea salts (derived from seawater). With mirabilite precipitation in sea-ice formation at temperatures lower than ca. -9 °C, molar ratios of the respective constituents relative to Na^+ can be raised gradually (e.g., Hara et al., 2012). The slopes in each regression line (Fig. 4) and the molar ratios of sea-salt constituents in frost flowers were larger than the seawater ratio found in this study. This implies that sea-salt fractionation occur in frost flowers. Moreover, the slopes for frost flowers were higher than those in brine except Cl^-. Precipitation of salts such as mirabilite and hydrohalite depend on temperature (Marion et al., 1999; Koop et al., 2000). Therefore, we attempted to compare relations of respective sea salts to

Cl^- and Mg^{2+} (Supplementary, Figures S2-S4). Relations among Mg^{2+}, K^+, Ca^{2+}, and Cl^- in frost flowers well matched those in brine. The molar ratios to Cl^- were not changed by mirabilite precipitation without Cl^- loss by heterogeneous reactions. However, the slopes of Mg^{2+}-Na^+, K^+-Na^+, and Ca^{2+}-Na^+ in brine were slightly higher than the seawater ratio. Similar to the slopes of frost flower, slopes of K^+-Na^+, and Ca^{2+}-Na^+ in snow on sea-ice were higher than seawater ratios. The slope of Mg^{2+}-Na^+, however, was lower than the seawater ratio, although fresh snow samples with the Na^+ concentration lower than 0.1 mmol L^{-1} were distributed on the seawater ratios. Figure 4 and Table 1 show that the molar ratios in frost flowers, brine, and snow varied depending on sampling sites, circumstances such as temperature, and the age of frost flowers (details are discussed later herein). The molar ratios in frost flowers resembled the ratios found by previous studies of frost flowers and aerosols (Rankin et al., 2002; Douglass et al., 2012; Hara et al., 2012). The Br^-/Na^+ ratios found from previous investigations, however, were varied considerably at frost flower sampling sites (Rankin et al., 2002; Alvarez-Aviles et al., 2008; Douglass et al., 2012). Br^- enrichment in frost flowers was observed in this study and previous studies conducted in the Weddell Sea, Antarctica by Rankin et al. (2002), although Alvarez-Aviles et al. (2008) and Obbard et al. (2009) reported that Br^- was not enriched in frost flowers (similar to the seawater ratio) at Barrow, Alaska and at Hudson Bay, Canada.

3.4 Aging of frost flowers and brine on sea ice

Figure 5 presents variations of CF_{Na} and molar ratio of SO_4^{2-}/Cl^- in frost flowers at Site I. As described above, aged frost flowers, young frost flowers, and fresh frost flowers were collected respectively at Site I, Site II, Site IIIa, and Site IIIb. The values of CF_{Na} of all samples exceeded 1.0, even on new ice at Site III, indicating that concentrated brine was excluded from sea ice to the sea-ice surface during sea-ice formation before the formation of frost flowers (Fig. 5a). Some samples with low CF_{Na} at Site I and II can be contaminated with slight snowfall. The CF_{Na} of frost flowers at Site III area was lower than that at Sites I and II, which suggests that sea-salt concentrations and sea-salt ratios of frost flowers varied depending on age of frost flowers and sea-ice.

To compare changes of sea-salt constituents with the aging of frost flowers, we attempted to monitor the sea-salt constituents of frost flowers and brines at Site I on 20–28 February, 2014. Figure 6 depicts short-term variations of air temperatures measured by AWS (T_{AWS}), air temperature above frost flowers (T_{air}, ca. 10 cm above the brine/sea-ice surface), temperature at bases of frost flowers (T_{FF}), and molar ratios of sea salts (SO_4^{2-}/Na^+, SO_4^{2-}/Cl^-, Br^-/Cl^-, I/Cl^-, Mg^{2+}/Cl^-, K^+/Cl^-, and Ca^{2+}/Cl^-) in frost flowers and brine. Unfortunately, we did not measure T_{air} and T_{FF} on 20–22 February. T_{AWS} on 20–28 February was lower than the temperature for mirabilite formation (ca. -9°C). In addition, T_{FF} was -18.9 – -21.3 °C on 24–28 February. In spite of the non-significant change of molar ratios of SO_4^{2-}/Na^+ and SO_4^{2-}/Cl^- in frost flowers on 26 February, other sea-salt ratios (Mg^{2+}/Cl^-, K^+/Cl^-, and Ca^{2+}/Cl^-) increased remarkably. Figure 6a shows that T_{AWS} and T_{air} had been lower than -25 °C since 23 February. Sea-salt ratios in brines at Site I were distributed along with seawater ratios. They varied non-significantly, although the ratios of Mg^{2+}/Cl^-, K^+/Cl^-, and Ca^{2+}/Cl^- were slightly higher than their respective seawater ratios. In contrast to the ratios in brines, molar ratios of SO_4^{2-}/Na^+ and SO_4^{2-}/Cl^- in frost flowers dropped greatly relative to seawater ratios. Molar ratios of Br^-/Cl^- and I/Cl^- in frost flowers were higher than the seawater ratio (values in literature) and brine (Figs. 6d–6e). As described above, Br^- and I were enriched in frost flowers at Site I. Although ratios of Mg^{2+}/Cl^-, K^+/Cl^-, Ca^{2+}/Cl^-, and Br^-/Cl^- increased on 26–28 February, increases in the ratio of I/Cl^- were not clear.

3.5 Morphology of sea-salt particles

Figure 7 depicts SEM images of aerosol particles collected above the sea-ice area with frost flowers. Most coarse aerosol particles collected on 1 March 2014 had structures with cuboid-crystal like materials (bright color in SEM image) and non-

crystal materials (gray – dark gray color in SEM image) around the cuboid-crystal like materials. Furthermore, most aerosol particles had stains around the particles. The presence of stains is direct evidence that the aerosol particles had a liquid surface in the atmosphere. In other words, the particles were deliquescent in the atmosphere. Na, Cl, and Mg were detected in aerosol particles of this type. Therefore, the particles might be identified as sea-salt particles. Strong peaks of Na and Cl were identified from cuboid-crystal like materials, whereas strong peaks of minor sea salts such as Mg, K, and S were also obtained from non-crystal materials. Depending on the amount (mass) of sea salts and water in a sea-salt particle, salts with lower solubility can exist in a state with a solid core. In SEM observations, however, aerosol particles were exposed to high vacuum conditions. They dried up. The localization of each sea salt in a particle might proceed in a high vacuum chamber. Therefore, it is noteworthy that the salt distribution in an SEM image differed from the state in the ambient atmosphere.

3.6 Elemental compositions of sea salts and relating salts in each aerosol particle

Figure 8 depicts EDX spectra of sea-salt particles and sea-salt-related particles in aerosol particles collected over the sea ice. In accordance with procedures of aerosol classification presented by Hara et al. (2013, 2014) and atomic ratios of the respective particles, the mixing states of sea-salt particles and related salt particles were classified into the following types: (1) sea-salt particles having atomic ratios similar to those of seawater (Fig. 8a); (2) Mg-rich sea-salt particles (Fig. 8b); (3) K-rich sea-salt particles (Fig. 8c); (4) modified sea-salt particles with a slight Cl-loss (Fig. 8d); (5) wholly modified sea-salt particles (Fig. 8e); (6) sea-salt particles internally mixed with mineral elements such as Al and Si (Fig. 8f); (7) Na_2SO_4 particles without Mg (Fig. 8g); (8) $MgCl_2$ particles (Fig. 8h); (9) $MgSO_4$ particles (Fig. 8i); and (10) KCl particles (Fig. 8j). Figure S6 shows that Mg in sea-salt particles might be present as $MgCl_2$. Actually, Mg and S were detected from aerosol particles in Fig. 8i. Atomic ratios of Mg and S of the aerosol particles containing only Mg and S were approximately compatible with $MgSO_4$. Actually, Mg-rich sea-salt particles, K-rich sea-salt particles, Mg-salt particles, and K-salt particles were identified also in the boundary layer over Syowa Station, Antarctica during winter–spring (Hara et al., 2013a) and near the surface on the Antarctic plateau during summer (Hara et al., 2014). Additionally, aerosol particles with atomic ratios similar to $CaCO_3$ were observed in the same aerosol samples (shown in *Supplementary Materials*, Fig. S7). In this study, these particles were observed only in aerosol samples collected near new sea ice. In addition, aerosol particles containing sulfates, minerals, soot, and anthropogenic metals were observed in this study.

3.7 Abundance of sea-salt particles and sea-salt-related particles

For quantitative discussion, the relative abundance was estimated from the results of EDX analyses (Fig. 9). In this study, sea-salt and modified sea-salt particles were major components of the coarse mode. High abundance of sea-salt particles corresponded to strong winds, high aerosol number concentrations, and appearance of low clouds (fog) above open sea off Siorapaluk. Although a few samples showed low relative abundance of sea-salt particles and modified sea-salt particles, this result corresponded to high relative abundance of minerals and minerals containing sulfates. However, it is noteworthy that the low number concentrations in coarse mode in the atmosphere engender low number density on the sample substrates and engender high uncertainty. For number concentrations of less than 10 L^{-1} in $D_p > 2.0$ μm, the number of the analyzed particles in coarse mode was several to approximately 16 particles.

Aerosol particles containing sulfates were dominant in fine mode, whereas sulfate particles were observed rarely in coarse mode. Relative abundance of nss-sulfate particles in fine mode were similar to that of the Arctic boundary layer around Svalbard (Hara et al., 2003). Relative abundance of sulfate particles in fine mode was higher under conditions with low wind speed and low aerosol number concentrations. The relative abundance of sea-salt particles and modified sea-salt particles in fine mode showed higher abundance than 40% under conditions with strong winds or high aerosol number concentrations in coarse mode.

3.8 Sea-salt fractionation of aerosol particles in coarse and fine modes

Figure 10 presents ternary plots of sea-salts (Na, Mg, and S) and Mg-rich sulfates in coarse and fine modes. Internal mixtures of sea salts and minerals were excluded from the ternary plots. The sum of the atomic ratios of Na, S and Mg in each sea-salt particle was not 100% in the most cases. Therefore, we converted sum of the atomic ratios to 100% for ternary plots. Labels of A, B, C, and D respectively denote the bulk seawater ratio, wholly Cl released sea-salt particles by SO_4^{2-}, wholly Na replaced sea-salts (close to $MgCl_2$), and sea-salts (close to $MgSO_4$) with wholly Cl release of SO_4^{2-} and wholly Na replacement by Mg. When the sea-salt particles are modified by sulfates and are not fractionated, they are distributed around the stoichiometric line of A-B. Mg in sea-salt particles can be enriched gradually with sea-salt fractionation by precipitation of mirabilite (Na_2SO_4 $10H_2O$) and hydrohalite (NaCl $2H_2O$) (Hara et al., 2012). When sea-salt fractionation (replacement between Na and Mg) occurs without sea-salt modification by sulfate, sea-salt particles are distributed around the stoichiometric line of A-C. When sea-salt fractionation and sea-salt modification by sulfate occur stoichiometrically and simultaneously, sea-salt particles are distributed around the stoichiometric line of A-D. Na-Mg-S ratios of frost flowers and brine were distributed around bulk seawater ratio (a), although slight Mg-enrichment was recognized in this study.

The Mg ratios in coarse aerosol particles collected near new sea ice (Site IIIa) on 3 March were distributed mainly around the bulk seawater ratio and $NaSO_4$ ratio (Fig. 10a). Mg was enriched slightly in some sea-salt particles, even in coarse modes. In contrast to the sea-salt particles, Mg-free particles were distributed around Na_2SO_4 ratio, as depicted in Fig. 8g. As described above, these particles distributed around Na_2SO_4 ratio (B) might be mirabilite particles. In fine mode, most of the sea-salt particles were distributed between the stoichiometric lines between seawater ratio – $MgSO_4$ and seawater – $MgCl_2$. Compared to the Mg ratio in coarse mode, Mg enrichment was obtained remarkably in fine sea-salt particles.

Although most of the sea-salt particles in coarse mode were distributed around the bulk seawater ratio on 14 January and 21 February, 2014 (Figs. 10 b-c), some coarse sea-salt particles had strong Mg-enrichment and were distributed around the stoichiometric line of seawater ratio – $MgCl_2$. A few particles showed atomic ratios that were roughly equal to that of $MgCl_2$. Similarly to coarse sea-salt particles, Mg enrichment was also identified in fine mode on 14 January and 21 February, 2014. However, Mg-rich sea-salt particles lay approximately midway between stoichiometric lines of seawater ratio-$MgCl_2$ and seawater ratio-$MgSO_4$. Moreover, $MgSO_4$ particles were identified occasionally in this study (e.g., 21 February, 2014).

In contrast to sea-salt particles on 14 January, 21 February, and 3 March, 2014, sea-salt particles in both modes were distributed mostly around the seawater ratio under the storm conditions with blowing and drifting snow on 1 March, 2014 (Fig. 10d), although some sea-salt particles in coarse and fine modes had slight Mg enrichment. Winds came not from young sea-ice area with frost flowers (Site I and II) but from old and very old sea-ice areas.

3.9 Variations of the fractionated sea-salt particles during winter

Figure 11 presents variations of Mg/Na ratios in sea-salt particles. Sea-salt particles internally mixed with mineral particles were excluded from Fig. 11 to avoid misunderstanding of the sea-salt chemistry. Mg/Na ratios were higher than the bulk seawater ratio (Mg/Na ≈ 0.11) in coarse and fine sea-salt particles during measurements. In conditions with blowing or drifting snow and strong winds, the Mg/Na ratios and the standard deviation decreased in both modes. However, higher Mg/Na ratios were observed in the calm wind conditions. Furthermore, Mg/Na ratios in coarse sea-salt particles increased gradually on DOY = 52–57 (22–27 February), when the air temperature was below -25 °C and the wind speed was lower than 4 m s^{-1}. After the storm on 1 March, Mg/Na ratios of sea-salt particles were distributed around the seawater ratio, although the ratios varied. In contrast to coarse sea-salt particles, Mg/Na ratios were higher in fine modes in this study. Similar tendencies were observed for aerosol particles over Syowa Station, coastal Antarctica (Hara et al., 2013), and on the Antarctic continent (Hara et al.,

2014). This size dependence of Mg enrichment of sea-salt particles is important to elucidate the processes of sea-salt particle release from sea ice and frost flowers.

4. Discussion

4-1. Sea-salt fractionation on sea-ice

Higher slopes of the sea-salt ratios relative to Na^+ (Fig. 4) and lower SO_4^{2-}/Na^+ ratio in frost flower (Fig. 5) strongly suggest that sea-salt fractionation such as mirabilite precipitation occurred on sea ice. Precipitation of salts such as mirabilite and hydrohalite depend on temperature (Marion et al., 1999; Koop et al., 2000). Therefore, we attempted to compare the relations of respective sea salts to Cl^- and Mg^{2+} (Supplementary, Figures S1 and S2). Relations among Mg^{2+}, K^+, Ca^{2+}, and Cl^- in frost flowers well matched those in brine. The molar ratios to Cl^- were not changed by mirabilite precipitation without Cl^- loss by heterogeneous reactions. However, frost flowers were more likely to be richer in Br^- and I^- than in Cl^- and Mg^{2+} (Table 1, Figs. S2-S4). Considering that the first step of precipitation of Na salt is mirabilite precipitation approximately at -9 °C, the coincidence of the relations of among Mg^{2+}, K^+, Ca^{2+}, and Cl^- suggests that enrichment of Mg^{2+}, K^+, and Ca^{2+} in frost flowers was driven mainly by mirabilite precipitation. The enrichment of Br^- and I relative to Cl^- and Mg^{2+} implies that Br^- and I were enriched somehow, but not by precipitation of mirabilite and hydrohalite.

When hydrohalite precipitation occurs under colder conditions, the molar ratios to Cl^- can rise in brine and frost flowers. As presented in Table 1, and Figures S2 and S4, the molar ratios to Cl^- in some brine samples markedly exceeded the seawater ratios. Therefore, sea-salt fractionation by hydrohalite might be promoted in some samples of brine and frost flowers. Similar to Mg^{2+}, K^+, Ca^{2+}, and Cl^-, Br^- and I can be enriched in frost flowers and brine by the precipitation of mirabilite and hydrohalite. The plausible processes for enrichment of Br^- and I can be listed as follows; (1) sea-salt fractionation by precipitation of salts containing Mg^{2+} or Cl^- and (2) surface enrichment of Br^- and I in liquid phase (e.g., brine). $MgCl_2$ and $MgSO_4$ were identified in aerosol particles as shown in Figs. 8 and S5. Considering presence of $MgCl_2$ and $MgSO_4$ in aerosol particles, Mg salts might be localized or precipitated in frost flowers and the slush layer. According to earlier laboratory and model studies (e.g., Mairon et al., 1999), $MgCl_2$ $6H_2O$ and KCl (sylvite) can be precipitated respectively at approximately -36 °C and -34 °C. During the measurements, minimum air temperature (-34.1 °C) and temperature at the surface of slush layer (T_{FF}) were higher than the temperature at $MgCl_2$ $6H_2O$ precipitation. Therefore, $MgCl_2 \bullet 6H_2O$ precipitation might not occur during the measurements, although precipitation of mirabilite and hydrohalite can occur. These salts can be precipitated if a strong vertical temperature gradient near the surface leads the temperature at the brine surface or around the top of frost flowers to drop to the temperature of precipitation of sylvite and $MgCl_2$ $6H_2O$. However, the temperature at the brine surface or around the top of the frost flower might be higher than temperature that causes precipitation of sylvite and $MgCl_2$ $6H_2O$ during the measurements. Thus, precipitation of sylvite and $MgCl_2$ $6H_2O$ might not occur near surface of brine on sea ice. Consequently, enrichment of Br^- and I in frost flowers might derive from sea-salt fractionation to a greater degree than precipitation of mirabilite and hydrohalite. In addition to sea-salt fractionation by precipitation of mirabilite, hydrohalite, $MgCl_2$ $6H_2O$ and sylvite, a molecular dynamics (MD) simulation conducted by Jungwirth and Tobias (2001) predicted considerable surface enhancement of Br^- and I in alkaline halide solutions. Enrichment of Br^- and I might proceed in frost flowers and brine by this surface enhancement and sea-salt fractionation if Br^- and I are preferably enhanced at the brine surface.

4-2. Aging of frost flowers and sea-salt fractionation

Molar ratios SO_4^{2-}/Cl^- in frost flowers at Sites I and II (Fig. 5b) were considerably lower than the seawater ratio. This change of SO_4^{2-}/Cl^- ratios might be attributed to sea-salt fractionation by sulfate depletion (i.e., mirabilite precipitation). By contrast, SO_4^{2-}/Cl^- ratios at Site III were similar to the seawater ratio. The distribution of SO_4^{2-}/Cl^- ratios implies strongly that (1) sea-

salt fractionation (e.g., mirabilite formation) occurs to a non-significant or slight degree on new sea-ice at Site III, and (2) mirabilite precipitation occurred in the new sea-ice stage. Considering direct evidence that mirabilite-like particles were identified only at Sites IIIa and IIIb, mirabilite might be precipitated on frost flowers in the early stage. Details of mirabilite-like particles were discussed in section of 4-3.

At Site I, sea-salt ratios changed gradually with growth and aging of frost flowers, as shown in Figure 6. Considering that T_{air} and T_{FF} were sufficiently low to allow progress of sea-salt fractionation such as precipitation of mirabilite and hydrohalite, these salts might be localized not in brine but on the solid surface of sea-ice and snow. Therefore, the lower ratios of SO_4^{2-}/Na^+ and SO_4^{2-}/Cl^- in frost flowers might be attributed to mirabilite formation. With sulfate depletion, ratios of Mg^{2+}/Cl^-, K^+/Cl^-, and Ca^{2+}/Cl^- increased from 20 February to 24 February. Actually, T_{FF} dropped approximately to the temperature for hydrohalite precipitation (ca. -22 °C). Therefore, this drastic change of the sea-salt ratios on 26 February might be associated with hydrohalite precipitation. T_{FF} was lower than the temperature at precipitation of mirabilite and hydrohalite and higher than those at precipitation of sylvite, $MgCl_2\ 6H_2O$, and $NaBr\ 5H_2O$ (e.g., Marion, 1999; Koop et al., 2000). Therefore, mirabilite and hydrohalite were precipitated in the slush layer and frost flowers. However, Mg salts such as $MgCl_2\ 6H_2O$ and $MgSO_4$ cannot be precipitated. Therefore, Mg might be enriched in the residual brine. In contrast to T_{FF}, T_{air} increased slightly on 26–27 February. Then it increased greatly on 28 February – 1 March. In spite of the slight increase of T_{AWS} and T_{air}, T_{FF} tended to decrease slightly on 24–27 February. This decrease of T_{FF} might be attributed to the reduction of heat conduction by sea-ice growth (larger thickness). Consequently, the sea-ice thickness might be a fundamentally important factor for sea-salt fractionation on sea ice, in addition to T_{air}. It is noteworthy that molar ratios in frost flowers cannot change if sea-salt fractionations such as mirabilite and hydrohalite precipitation occur on frost flowers after brine migration onto frost flowers. Whether mirabilite and hydrohalite were precipitated on frost flowers or not, the total amount (mass) of precipitated salts and sea salts in residual brine did not change without liberation by heterogeneous reactions. Although halides (Cl^-, Br^-, and I) can be released from frost flowers, Mg^{2+}, K^+, and Ca^{2+} cannot be released by heterogeneous reactions. Suggesting (1) considerable change of the molar ratios in frost flowers, (2) non-significant change of those in brine, and (3) T_{FF} close to ca. -21 °C, precipitation of mirabilite and hydrohalite might be driven near the surface of brine on the sea ice. Then, the residual brine might be migrated vertically onto frost flowers. Because of the strong vertical gradient of the air temperature near the surface of the sea ice and frost flowers, subsequent sea-salt fractionation can proceed near the tips of frost flowers under colder conditions.

To elucidate halogen chemistry in frost flowers, we compared features of Br^-/Cl^- and I/Cl^- in frost flowers at Site I. High correlation of Cl^--Na^+ and Cl^- enrichment strongly suggests that Cl^- release was non-significant from frost flowers and brine. Therefore, we specifically examine the features of Br^- and I here. we attempt to estimate the molar ratios of Br^-/Cl^- and I/Cl^- in frost flowers using the ratios of Mg^{2+}/Cl^-, Br^-/Cl^- and I/Cl^- on 22–26 February, assuming that hydrohalite was not precipitated yet on 22–26 February, and that Br^- and I did not liberate from frost flowers through heterogeneous reactions. When the molar ratios on 22–26 February changed by the assumptions above, the molar ratios of Br^-/Cl^- and I/Cl^- in frost flowers after hydrohalite precipitation were estimated respectively as 0.00214 and 1.82×10^{-6}. Although the Br^-/Cl^- ratio (0.00206) on 27 February was slightly lower than the estimated ratio, this difference might be very slight or non-significant. Therefore, Br^- release from frost flowers might be non-significant at Site I under dusk conditions. However, the estimated I/Cl^- ratio on 27 February was higher than the ratios in frost flowers (1.562×10^{-6}). The following likelihood should be considered: (1) reduction of I enrichment by precipitation of salts containing iodine, and (2) I release from frost flowers through heterogeneous reactions. Although $NaBr{\bullet}5H_2O$ can be precipitated at -28 °C (Koop et al., 2000), no report in the relevant literature describes a study of precipitation of iodine salts in sea salts. This difference implies the likelihood that I was released from frost flowers if iodine

salts were not precipitated under the conditions at Site I. Iodine can be released from frost flowers through the following heterogeneous reactions (Thompson and Zafiriou, 1983; Carpenter, 2003; Simpson et al., 2007; Saiz-Lopez et al., 2015).

$$HOI + Br^- + H^+ \rightarrow IBr + H_2O \quad (R1)$$

$$I^- + H_2O_2 \rightarrow HOI + OH^- \quad (R2)$$

$$HOI + I^- + H^+ \rightarrow I_2 + H_2O \quad (R3)$$

$$I^- + O_3 + H_2O \rightarrow HOI + O_2 + OH \quad (R4)$$

Reactions of R4 can proceed under nighttime conditions. Other reactions, however, are enhanced under conditions with solar radiation because HOI can be formed efficiently through atmospheric photochemical reactions. Frost flowers at Site I had been exposed to direct solar radiation since 18 February, 2014, although it had been dusk at noon since early February. Therefore, the heterogeneous iodine loss from frost flowers can engender reduction of I enrichment after hydrohalite precipitation in frost flowers. From the I/Cl^- ratios, amount of the released iodine from frost flowers can be estimated to ca. 16 % under our research conditions. The more solar radiation, the more reactive halogens might be released from frost flowers and brines. Comparing the short-term features of Br^-/Cl^- and I/Cl^- in frost flowers, heterogeneous I loss appears likely to occur from frost flowers relative to heterogeneous Br^- loss.

4-3. Fractionated sea-salt particles in the atmosphere

Mg was enriched in sea-salt particles collected in this study. The following evidence is important to elucidate the origins of Mg-rich sea-salt particles and Mg-rich salt particles in the atmosphere: (1) presence of highly Mg-rich particles (Mg-rich sea-salts, $MgCl_2$, and $MgSO_4$), (2) T_{FF} lower than temperature at precipitation of mirabilite and hydrohalite, (3) higher Mg/Na ratio in fine mode, and (4) small variation of the Mg/Na ratio in strong winds and blowing snow. Mg-rich sea-salts and Mg-salts cannot be evaporated or vaporized under ambient conditions. Therefore, these particles must be released through physical processes. Sea-salt fractionation can occur if sea-salt particles are fractured in the atmosphere. However, direct evidence of fracture of sea-salt particles in the atmosphere has not been obtained (Lewis and Schwartz, 2004).

With sea-salt fractionation in brine and frost flowers, sea-salt particles released from sea-ice were found to have different sea-salt ratios from those of seawater, as discussed above. Actually, Mg^{2+}, K^+ and Ca^{2+} were enriched in frost flowers and the residual brine. Therefore, Mg-rich sea-salt particles (Fig. 8b), K-rich sea-salt particles (Fig. 8c), Mg-salt particles (Figs. 8h–8i), and K-salt particles (Fig. 8j) might originate from the sea-ice area and might be associated with sea-salt fractionation. Although sea-salts in the brine and frost flowers were fractionated through precipitation of mirabilite and hydrohalite, SO_4^{2-} depletion by mirabilite precipitation was identified only to a slight degree in sea-salt particles because of the heterogeneous SO_4^{2-} formation (*Supplementary information, Figs. S8-S9*). In aerosol particles in Fig. 8g, Na and S were detected, but not Mg. Mg ratios in coarse sea-salt particles exceed the usual detection limit of single particle analysis by EDX. Therefore, the aerosol particles might have an extremely poor Mg ratio. The atomic ratios of Na and S of the Mg-poor particles imply strongly that the particles were in the form of Na_2SO_4. If the sea-salt particles were modified with SO_4^{2-} by heterogeneous reactions, then the modified sea-salt particles contained sea-salt Mg. Consequently, the presence of Na_2SO_4 particles cannot be explained by their release from the sea surface. The Mg-free sulfate particles might therefore not be the modified sea-salt particles. Na_2SO_4 particles were observed only at Sites IIIa and IIIb. Simultaneously, $CaCO_3$-like particles were identified at Sites IIIa and IIIb. In the early stage of sea-ice formation, ikaite ($CaCO_3$ $6H_2O$) and mirabilite (Na_2SO_4 $10H_2O$) can be precipitated respectively at -2°C and -8.8 °C on/in sea ice (Dieckmann et al., 2008, 2010; Marion et al., 1999). Therefore, these particles might be mirabilite-like and ikaite-like particles.

The Mg/Na ratios in sea-salt particles varied greatly depending on the sampling site and meteorological conditions (e.g., winds and temperature) as presented in Fig. 11. Variations of Mg/Na ratios in sea-salt particles are extremely interesting to elucidate the release processes of sea-salt particles from the sea-ice surface. It is noteworthy that sea-salt particles at Sites IIIa and IIIb were distributed around seawater ratios. Therefore, sea-salt particles except mirabilite-like and ikaite-like particles at Site IIIa and IIIb might be released from the sea surface. Such particles had been present at Sites IIIa and IIIb since 2 March. Moreover, the presence of ikaite-like particles and mirabilite-like particles in the atmosphere implies that these particles were released into the atmosphere from the early stage of sea ice after precipitation of ikaite and mirabilite on sea-ice and frost flowers. As described above, SO_4^{2-}/ Cl^- ratios in fresh frost flowers at Sites IIIa and IIIb were similar to the seawater ratio (Fig. 5). Furthermore, frost flowers were wet because of the brine migration. Therefore, mirabilite might be present (precipitated) in brine and on frost flowers in the early stage of sea-ice formation. Higher Mg/Na ratios in sea-salt particles (except Sites IIIa and IIIb) suggest strongly that Mg-rich sea-salt particles were supplied from the sea-ice area to the atmosphere. As shown in Figure 4, Mg^{2+}/Na^+ ratios in frost flowers at Site I increased gradually on 20 February – 1 March under colder conditions. The correspondence between high Mg/Na ratios in coarse mode and the coldest conditions implies strongly that Mg/Na ratios in coarse sea-salt particles responded rapidly to sea-salt fractionation on sea ice and frost flowers. If sea salts were distributed homogeneously on and in sea ice, frost flowers, and brine, then the size dependence of Mg enrichment might not occur in sea-salt particles released from sea-ice areas. Therefore, high Mg enrichment in fine mode strongly suggests the localization of Mg salts on and in the residual brines, sea ice and the frost flowers, in addition to the preferential release of fine aerosol particles containing Mg-rich salts from sea ice and frost flowers.

High aerosol number concentrations and high abundance of sea-salt particles with Mg enrichment under strong winds implies that sea-salt particles were dispersed from the sea-ice surface. Although high aerosol number concentrations were observed occasionally at Siorapaluk under calm winds, the features might result from transport of (1) sea-salt particles released elsewhere by strong winds and (2) anthropogenic aerosols (i.e., sulfates and Arctic haze). Because of the high abundance of sea-salt particles, most cases of higher aerosol number concentrations in calm winds were likely associated with the release and transport of sea-salt particles. Similar phenomena were identified also at the Antarctic coasts (Hara et al., 2010). Under conditions with blowing snow and strong winds, sea-salt particles were released from the sea-ice area, as reported from earlier works (e.g., Hara et al., 2004, 2012). Earlier investigations (Obbard et al., 2009; Roscoe et al., 2011) have shown, however, that aerosol particles were released non-significantly by the breakage of frost flowers under strong winds. Therefore, Mg-rich sea-salt particles and Mg-rich salt particles might be released by processes other than breakage of frost flowers. Strong winds can engender the release of smaller ice particles containing solid sea-salts and brine from sea-ice areas by erosion of snow and slush layers, and by splash of brine. Indeed, the variation of Mg/Na ratios in sea-salt particles was smaller in both coarse and fine modes under strong winds (DOY = 40 and 59), although surface winds passed from very-old and old sea-ice areas that were patchily covered with snow (absence of slush layer) to sampling sites (Fig. 11). In other words, this result suggests that Mg-rich sea-salt particles were released also from snow layer on old and very-old sea ice through erosion of snow by strong winds, and suggests that highly Mg-rich sea-salt particles and Mg-salts were released non-significantly from old- and very-old sea-ice areas. By contrast, Mg/Na ratios were varied largely under calm wind conditions. To explain the presence of highly Mg-rich sea-salt particles and Mg-rich salt particles, we speculated that these particles were released from the residual brine through splashing of brine in the slush layer and shattering of brine films on frost flowers and snow. Indeed, Mg depletion was observed in the aged snow on the slush layer. If fine sea-salt particles were released from the residual brine on frost flowers, slush layers, and snow, then higher Mg/Na ratios in fine sea-salt particles are eminently explainable. To elucidate these points, we must accumulate more information related to the salt distribution on and in frost flowers and sea ice at the nanometer–micrometer scale.

5. Concluding remarks

Simultaneous sampling and observations of frost flowers, brines, and atmospheric aerosol particles were conducted around Siorapaluk, north-western Greenland at the end of December, 2013 – early March 2014. We obtained the following direct evidence from our field observations: (1) presence of ikaite-like particles, mirabilite-like particles, and sea-salt particles with ratios similar to seawater in the atmosphere at new sea-ice areas (Sites IIIa and IIIb); (2) changes of sea-salt ratios of frost flowers by sea-salt fractionation at Site I; and (3) presence of Mg-rich sea-salt particles and Mg-salt particles in the atmosphere. From this evidence and results from earlier works, we propose the following as hypotheses for the processes of sea-salt fractionation on sea-ice and the release of sea-salt particles into the atmosphere (Fig. 12).

Initial stage: open sea surface

Before sea-ice formation, sea-salt particles are released from the sea surface through bubble bursting and breaking waves (e.g., Lewis and Schwartz, 2004). Sea-salt ratios in the particles are similar to the seawater ratio.

First stage: seawater freezing

Seawater starts freezing at lower air temperatures. In this stage, sea-ice was present as conditions of grease-ice, frazil ice, and sludge. Considering that sea-salt particles with ratios similar to seawater were found to be present only at Sites IIIa and IIIb, these particles must be released from the sea surface in the initial stage and first stage. Depending on the temperature at the sea-ice surface, ikaite starts precipitation because ikaite precipitation temperatures are higher than that of mirabilite.

Second stage: sea-ice formation and sea-salt fractionation

Then, the sea-surface was covered with thin sea-ice as at Sites IIIa and IIIb. Presence of sea ice prevents the release of sea-salt particles from the sea surface to the atmosphere. A strong vertical gradient of air temperature near the sea-ice surface caused frost flower formation. Some brine is migrated on frost flowers. Cooling of the frost flower surface and brine can engender precipitation of ikaite and mirabilite. Ikaite-like and mirabilite particles are released from frost flowers and brine on sea-ice into the atmosphere. Ikaite-like particles and mirabilite-like particles are released into the atmosphere.

Third stage: frost flower growth and sea-salt fractionation

With sea-ice growth, the temperature on sea-ice (T_{FF}) decreases gradually by reduction of heat conduction from seawater to the sea-ice surface. Lower temperatures on and in the slush layer induce sea-salt fractionation by precipitation of mirabilite and hydrohalite. Sea-salt enrichment (e.g., Mg^{2+}, K^{+}, Ca^{2+}, Br^{-} and iodine) proceeds gradually in the residual brine by Na-salt precipitation. The residual brine having Mg enrichment is migrated vertically on frost flowers. , $NaBr\ 5H_2O$, sylvite and $MgCl_2$ can be precipitated if the air temperature at the top of frost flowers decreases to approximately -33 °C by the vertical gradient. Mg-rich sea-salt particles and Mg-salts are released from the brine and surface snow. Iodine is released into the atmosphere through heterogeneous reactions and Br^{-} is released slightly or non-significantly under dusk conditions. The more solar radiation, the more reactive halogens can be released from frost flowers and brines.

Fourth stage: strong winds and snowfall on Frost flower

Under conditions with strong winds, snowfall, and blowing snow, snow particles were attached on frost flowers and slush layers. As suggested by laboratory experiments (Roscoe et al., 2010), aerosol particles are released non-significantly from frost flowers. However, Mg-rich sea-salt particles and Mg-salts are released from the brine and surface snow by winds.

Fifth stage: frost flower covered with snow

When snowfall and blowing snow are sufficient to cover frost flowers and the slush layer, frost flowers are buried completely in snow after the storm. Brine on sea-ice and frost flowers can be mixed into the snow layer. Sea-salt concentrations (salinity) in the brine layer gradually decrease by migration and mixing into the snow layer. As a result, the sea-ice surface (bottom of snow layer) freezes gradually. Sea-salts in the migrated brine and frost flowers can be redistributed through snow metamorphosis, although distributions of sea-salts might be heterogeneous in the snow layer.

Sixth stage: snow erosion by strong winds

Then, strong winds engender snow layer erosion. In other words, Mg-rich sea-salt particles are released into the atmosphere. A dry and hard surface of sea ice appears after snow layers are removed completely.

We observed frost flowers and aerosols on sea-ice in the fjord near Siorapaluk. Therefore, we were able to compare each stage easily. If sea-ice areas having frost flowers are present in the locations affected by winds, waves, tides, and ocean currents (e.g., Arctic Ocean and Antarctic coasts), then sea-ice can flow out and have many cracks, which can appear often. Under such conditions, some stages might duplicate and proceed simultaneously. At the moment, some processes are inferred from our field evidence. In addition to analysis of frost flowers, more field studies and laboratory experiments must be applied to aging frost flowers, sea-salt fractionation, and the release of fractionated sea-salts into the atmosphere, and halogen chemistry in polar regions.

Acknowledgments

We thank Ikuo Oshima and Siorapaluk residents for extremely useful comments and help related to operations on sea ice, sea-ice conditions, and the appearance of frost flowers. This study was supported by a Grant-in-Aid for Challenging Exploratory Research (PI: K. Hara, No. 25550018).

References

Abbatt, J., Thomas, J., Abrahamsson, K., Boxe, C., Granfors, A., Jones, A., King, M., Saiz-Lopez, A., Shepson, P., Sodeau, J., Toohey, D., Toubin, C., Glasow, R., Wren, S., and Yang, X.: Halogen activation via interactions with environmental ice and snow in the polar lower troposphere and other regions, Atmospheric Chemistry and Physics, 12, doi:10.5194/acp-12-6237-2012, 2012.

Alvarez-Aviles, L., Simpson, W., Douglas, T., Sturm, M., Perovich, D., and Domine, F.: Frost flower chemical composition during growth and its implications for aerosol production and bromine activation, Journal of Geophysical Research, doi:10.1029/2008JD010277, 2008.

Barrie, L. A., Bottenheim, J. W., Schnell, R. C., and Crutzen, P. J.: Ozone destruction and photochemical reactions at polar sunrise in the lower Arctic atmosphere, Nature, 334, 138–141, doi:10.1038/334138a0, 1988.

Carpenter, L. J.: Iodine in the marine boundary layer, Chem. Rev., 103(12), 4953–4962, doi:10.1021/cr0206465, 2003.

Chen, Z., Megharaj, M., and Naidu, R.: Speciation of iodate and iodide in seawater by non-suppressed ion chromatography with inductively coupled plasma mass spectrometry, Talanta, 72(5), 1842–1846, doi:10.1016/j.talanta.2007.02.014, 2007.

Dieckmann, G. S., Nehrke, G., Papadimitriou, S., Göttlicher, J., Steininger, R., Kennedy, H., Wolf-Gladrow, D., and Thomas, D. N.: Calcium carbonate as ikaite crystals in Antarctic sea ice, Geophysical Research Letters, 35(8), doi:10.1029/2008GL033540, 2008.

Dieckmann, G., Nehrke, G. Uhlig, C., and Göttlicher, J: Ikaite ($CaCO_3$• $6H_2O$) discovered in Arctic sea ice, The Cryosphere, doi:10.5194/tc-4-227-2010, 2010.

Ding, Z. J., Li, Y. G., Zeng, R. G., Mao, S. F., Zhang, P., and Zhang, Z. M.: Depth distribution functions of secondary electron production and emission, J. Surface Anal., 15, 249–253, 2009.

Domine, F., Taillandier, A., Simpson, W., and Severin, K.: Specific surface area, density and microstructure of frost flowers, Geophysical Research Letters, 32(13), doi:10.1029/2005GL023245, 2005

Douglas, T., Domine, F., Barret, M., Anastasio, C., Beine, H., Bottenheim, J., Grannas, A., Houdier, S., Netcheva, S., Rowland, G., Staebler, R., and Steffen, A.: Frost flowers growing in the Arctic Ocean – atmosphere – sea ice – snow interface: 1. Chemical composition, Journal of Geophysical Research, 117, doi:10.1029/2011JD016460, 2012.

Ebinghaus, R., Kock, H., Temme, C., Einax, J., Löwe, A., Richter, A., Burrows, J., and Schroeder, W.: Antarctic Springtime Depletion of Atmospheric Mercury, Environmental Science & Technology, 36(6), 1238–1244, doi:10.1021/es015710z, 2002.

Foster, K. L., Plastridge, R. A., Bottenheim, J. W., Shepson, P. B., Finlayson-Pitts, B. J., and Spicer, C. W.: The role of Br2 and BrCl in surface ozone destruction at polar sunrise, Science, 291(5503), 471–474, doi:10.1126/science.291.5503.471, 2001.

Geilfus, N.-X., Galley, R., Cooper, M., Halden, N., Hare, A., Wang, F., Søgaard, D., and Rysgaard, S.: Gypsum crystals observed in experimental and natural sea ice, Geophysical Research Letters, doi:10.1002/2013GL058479, 2013.

Goldstein, J. I., Newbury, D. E., Joy, D. C., Lyman, C. E., Echlin, P., Lifshin, E., Sawyer, L., and Michael, J.: Chapter 6 Generation of X-rays in the SEM specimen, in: Scanning Electron Microscopy and X-ray Micronalysis, 3, 271–296, Plenum Press, New York, 2003.

Hara, K., Nakazawa, F., Fujita, S., Fukui, K., Enomoto, H., and Sugiyama, S.: Horizontal distributions of aerosol constituents and their mixing states in Antarctica during the JASE traverse, Atmospheric Chemistry and Physics, 14(18), 10211–10230, doi:10.5194/acp-14-10211-2014, 2014.

Hara, K., Osada, K., Hayashi, M., Matsunaga, K., Shibata, T., Iwasaka, Y., and Furuya, K.: Fractionation of inorganic nitrates in winter Arctic troposphere: Coarse aerosol particles containing inorganic nitrates, Journal of Geophysical Research, doi:10.1029/1999JD900348, 1999.

Hara, K., Osada, K., Kido, M., Hayashi, M., Matsunaga, K., Iwasaka, Y., Yamanouchi, T., Hashida, G., and Fukatsu, T.: Chemistry of sea-salt particles and inorganic halogen species in Antarctic regions: Compositional differences between coastal and inland stations, Journal of Geophysical Research, 109(D20), doi:10.1029/2004JD004713, 2004.

Hara, K., Osada, K., Kido, M., Matsunaga, K., Iwasaka, Y., Hashida, G., and Yamanouchi, T.: Variations of constituents of individual sea-salt particles at Syowa Station, Antarctica, Tellus B, 57(3), 230–246, doi:10.1111/j.1600-0889.2005.00142.x, 2005.

Hara, K., Osada, K., Yabuki, M., Hashida, G., Yamanouchi, T., Hayashi, M., Shiobara, M., Nishita, C., and Wada, M.: Haze episodes at Syowa Station, coastal Antarctica: Where did they come from?, Journal of Geophysical Research, 115(D14), doi:10.1029/2009JD012582, 2010.

Hara, K., Osada, K., Yabuki, M., and Yamanouchi, T.: Seasonal variation of fractionated sea-salt particles on the Antarctic coast, Geophysical Research Letters, 39(18), doi:10.1029/2012GL052761, 2012.

Hara, K., Osada, K., and Yamanouchi, T.: Tethered balloon-borne aerosol measurements: seasonal and vertical variations of aerosol constituents over Syowa Station, Antarctica, Atmospheric Chemistry and Physics, 13(17), 9119–9139, doi:10.5194/acp-13-9119-2013, 2013.

Hirokawa, T., Ichihara, T., Ito, K., and Timerbaev, A.: Trace ion analysis of seawater by capillary electrophoresis: determination of iodide using transient isotachophoretic preconcentration, Electrophoresis, 24(14), 2328–2334, doi:10.1002/elps.200305445, 2003.

Horikawa, Y., Kusumoto, R., Yamane, K., Nomura, R., Hirokawa, T., and Ito, K.: Determination of Inorganic Anions in Seawater Samples by Ion Chromatography with Ultraviolet Detection Using Monolithic Octadecylsilyl Columns Coated with Dodecylammonium Cation, Analytical Sciences, 32(10), 1123–1128, doi:10.2116/analsci.32.1123, 2016.

Ito, K.: Determination of Iodide in Seawater by Ion Chromatography, Analytical Chemistry, 69(17), 3628–3632, doi:10.1021/ac9700787, 1997.

Ito, K.: Semi-micro ion chromatography of iodide in seawater, Journal of Chromatography A, 830(1), 211–217, doi:10.1016/S0021-9673(98)00910-8, 1999.

Ito, K., Ichihara, T., Zhuo, H., Kumamoto, K., Timerbaev, A., and Hirokawa, T.: Determination of trace iodide in seawater by capillary electrophoresis following transient isotachophoretic preconcentration Comparison with ion chromatography, Analytica Chimica Acta, 497(1-2), 67–74, doi:10.1016/j.aca.2003.08.052, 2003

Jungwirth, P. and Tobias, D.: Molecular Structure of Salt Solutions: A New View of the Interface with Implications for Heterogeneous Atmospheric Chemistry, Journal of Physical Chemistry B, doi:10.1021/jp012750g, 2001.

Kaleschke, L., Richter, A., Burrows, J., Afe, O., Heygster, G., Notholt, J., Rankin, A., Roscoe, H., Hollwedel, J., Wagner, T., and Jacobi, H. W.: Frost flowers on sea ice as a source of sea salt and their influence on tropospheric halogen chemistry, Geophysical Research Letters, 31(16), doi:10.1029/2004GL020655, 2004.

Kelly, J. and Wexler, A.: Thermodynamics of carbonates and hydrates related to heterogeneous reactions involving mineral aerosol, Journal of Geophysical Research, doi:10.1029/2004JD005583, 2005.

Koop, T., Kapilashrami, A., Molina, L., and Molina, M.: Phase transitions of sea-salt/water mixtures at low temperatures: Implications for ozone chemistry in the polar marine boundary layer, Journal of Geophysical Research, 105(D21), 26393, doi:10.1029/2000JD900413, 2000.

Lewis, E. R., and Schwartz, S. E.: Measurements and Models of Quantities Required to Evaluate Sea Salt Aerosol Production Fluxes in "Sea Salt Aerosol Production: Mechanisms, Methods, Measurements and Models", American Geophysical Union, 2004, pp. 119–297.

Lieb-Lappen, R. M. and Obbard, R. W.: The role of blowing snow in the activation of bromine over first-year Antarctic sea ice, Atmospheric Chemistry and Physics, doi:10.5194/acp-15-7537-2015, 2015.

Lide, D. R., Handbook of Chemistry and Physics 86th edition, 2005.

Marion, G., Farren, R., and Komrowski, A.: Alternative pathways for seawater freezing, Cold Regions Science and Technology, 29(3), 259266, doi:10.1016/S0165-232X(99)00033-6, 1999.

Martin, S., Drucker, R., and Fort, M.: A laboratory study of frost flower growth on the surface of young sea ice, Journal of Geophysical Research: Oceans (1978–2012), 100(C4), doi:10.1029/94JC03243, 1995.

Martin, S., Yu, Y., and Drucker, R.: The temperature dependence of frost flower growth on laboratory sea ice and the effect of the flowers on infrared observations of the surface, Journal of Geophysical Research: Oceans, 1978 2012, 101(C5), doi:10.1029/96JC00208, 1996.

Millero, F., Feistel, R., Wright, D., and McDougall, T.: The composition of Standard Seawater and the definition of the Reference-Composition Salinity Scale, Deep Sea Research Part I: Oceanographic Research Papers, 55(1), 50–72, doi:10.1016/j.dsr.2007.10.001, 2008

Mochida, M., Hirokawa, J., and Akimoto, H.: Unexpected large uptake of O_3 on sea salts and the observed Br_2 formation, Geophysical Research Letters, 27(17), 2629–2632, doi:10.1029/1999GL010927, 2000.

Morin,S., Marion, G. M. and von Glasow, R., Voisin, D, Bouchez, J. and Savarino, J.: Precipitation of salts in freezing seawater and ozone depletion events: a status report, Atmos. Chem. Phys., 8, 7317–7324, 2008

Obbard, R., Roscoe, H., Wolff, E., and Atkinson, H.: Frost flower surface area and chemistry as a function of salinity and temperature, Journal of Geophysical Research, doi:10.1029/2009JD012481, 2009.

Perovich, D. and Richter-Menge, J.: Surface characteristics of lead ice, Journal of Geophysical Research: Oceans (1978–2012), 99(C8), doi:10.1029/94JC01194, 1994.

Rankin, A., Auld, V., and Wolff, E.: Frost flowers as a source of fractionated sea salt aerosol in the polar regions, Geophys. Res. Lett., doi:10.1029/2000GL011771, 2000.

Rankin, A., Wolff, E. and Martin, S.: Frost flowers: Implications for tropospheric chemistry and ice core interpretation, Journal of Geophysical Research, 107(D23), doi:10.1029/2002JD002492, 2002.

Roscoe, H., Brooks, B., Jackson, A., Smith, M., Walker, S., Obbard, R., and Wolff, E.: Frost flowers in the laboratory: Growth, characteristics, aerosol, and the underlying sea ice, Journal of Geophysical Research, doi:10.1029/2010JD015144, 2011.

Saiz-Lopez, A., Blaszczak-Boxe, C., and Carpenter, L.: A mechanism for biologically induced iodine emissions from sea ice, Atmos. Chem. Phys., 15(17), 9731–9746, doi:10.5194/acp-15-9731-2015, 2015.

Schroeder, W. H., Anlauf, K. G., Barrie, L. A., Lu, J. Y., and Steffen, A.: Arctic springtime depletion of mercury, Nature, 394, 331-332, 1998.

Simpson, W., Alvarez-Aviles, L., Douglas, T., Sturm, M., and Domine, F.: Halogens in the coastal snow pack near Barrow, Alaska: Evidence for active bromine air–snow chemistry during springtime, Geophysical Research Letters, 32(4), doi:10.1029/2004GL021748, 2005.

Simpson, W. R., von Glasow, R., Riedel, K., Anderson, P., Ariya, P., Bottenheim, J., Burrows, J., Carpenter, L. J., Frieß, U., Goodsite, M. E., Heard, D., Hutterli, M., Jacobi, H.-W., Kaleschke, L., Neff, B., Plane, J., Platt, U., Richter, A., Roscoe, H., Sander, R., Shepson, P., Sodeau, J., Steffen, A., Wagner, T., and Wolff, E.: Halogens and their role in polar boundary-layer ozone depletion, Atmos. Chem. Phys., 7, 4375-4418, doi:10.5194/acp-7-4375-2007, 2007.

Style, R. and Worster, M.: Frost flower formation on sea ice and lake ice, Geophysical Research Letters, doi:10.1029/2009GL037304, 2009.

Thompson, A. M. and Zafiriou, O. C.: Air-Sea Fluxes of Transient Atmospheric Species, J. Geophys. Res., 88, 6696–6708, doi:10.1029/JC088iC11p06696, 1983.

Udisti, R., Dayan U., Becagli S., Busetto M., Frosini D., Legrand M., Lucarelli F., Preunkert S., Severi M., Traversi R., and Vitale V.: Sea spray aerosol in central Antarctica. Present atmospheric behaviour and implications for paleoclimatic reconstructions, Atmos. Environ., 52, 109–120, 2012.

Wagenbach, D., Ducroz, F., Mulvaney, R., Keck, L., Minikin, A., Legrand, M., Hall, J., and Wolff, E.: Sea-salt aerosol in coastal Antarctic regions, Journal of Geophysical Research, doi:10.1029/97JD01804, 1998.

Wolff, E., Fischer, H., Fundel, F., Ruth, U., Twarloh, B., Littot, G., Mulvaney, R., Röthlisberger, R., de Angelis, M., Boutron, C., Hansson, M., Jonsell, U., Hutterli, M., Lambert, F., Kaufmann, P., Stauffer, B., Stocker, T., Steffensen, J., Bigler, M., Siggaard-Andersen, M., Udisti, R., Becagli, S., Castellano, E., Severi, M., Wagenbach, D., Barbante, C., Gabrielli, P., and Gaspari, V.: Southern Ocean sea-ice extent, productivity and iron flux over the past eight glacial cycles, Nature, 440, 491–496, doi:10.1038/nature04614, 2006.

Wolff, E. W., Rankin, A. M., and Röthlisberger, R.: An ice core indicator of Antarctic sea ice production, Geophys. Res. Lett., 30(22), 2158, doi:10.1029/2003GL018454, 2003.

Yang, X., Pyle, J. A., Cox, R. A., Theys, N. and van Roozendael, M.: Snow-sourced bromine and its implications for polar tropospheric ozone, Atmospheric Chemistry and Physics, 10(16), 7763-7773, doi:10.5194/acpd-10-8135-2010, 2010.

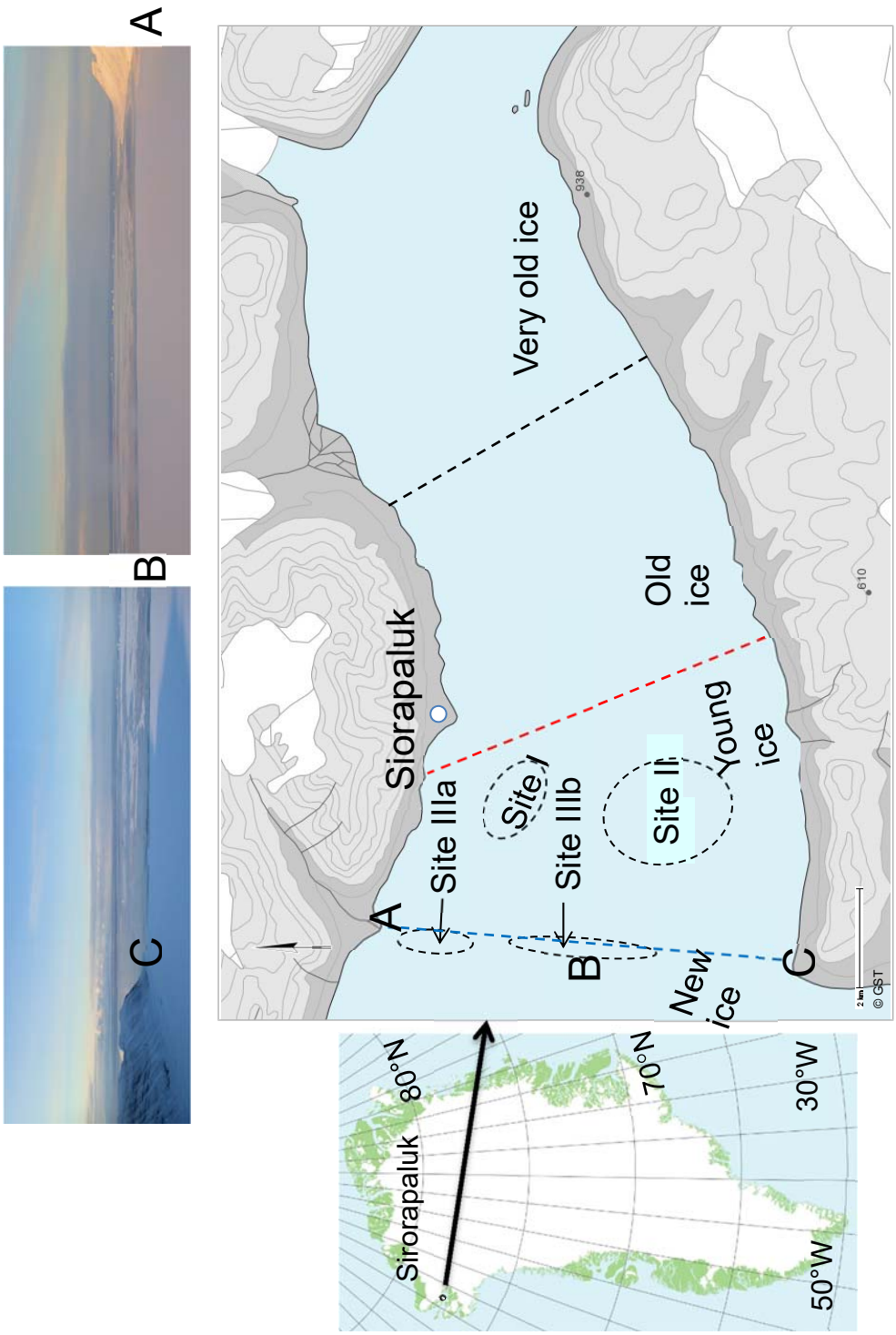

Figure 1 Locations of sampling and sea-ice conditions around Siorapaluk and photographs of new sea-ice conditions off Siorapaluk (taken from helicopter on 7 March, 2014). Black, red, and blue broken lines show locations of sea-ice break in November, 2013, and on 10-14 Feberuary, 2014, and 1 March, 2014, respectively. Marks of A, B, and C denote broad locations in maps and photographs.

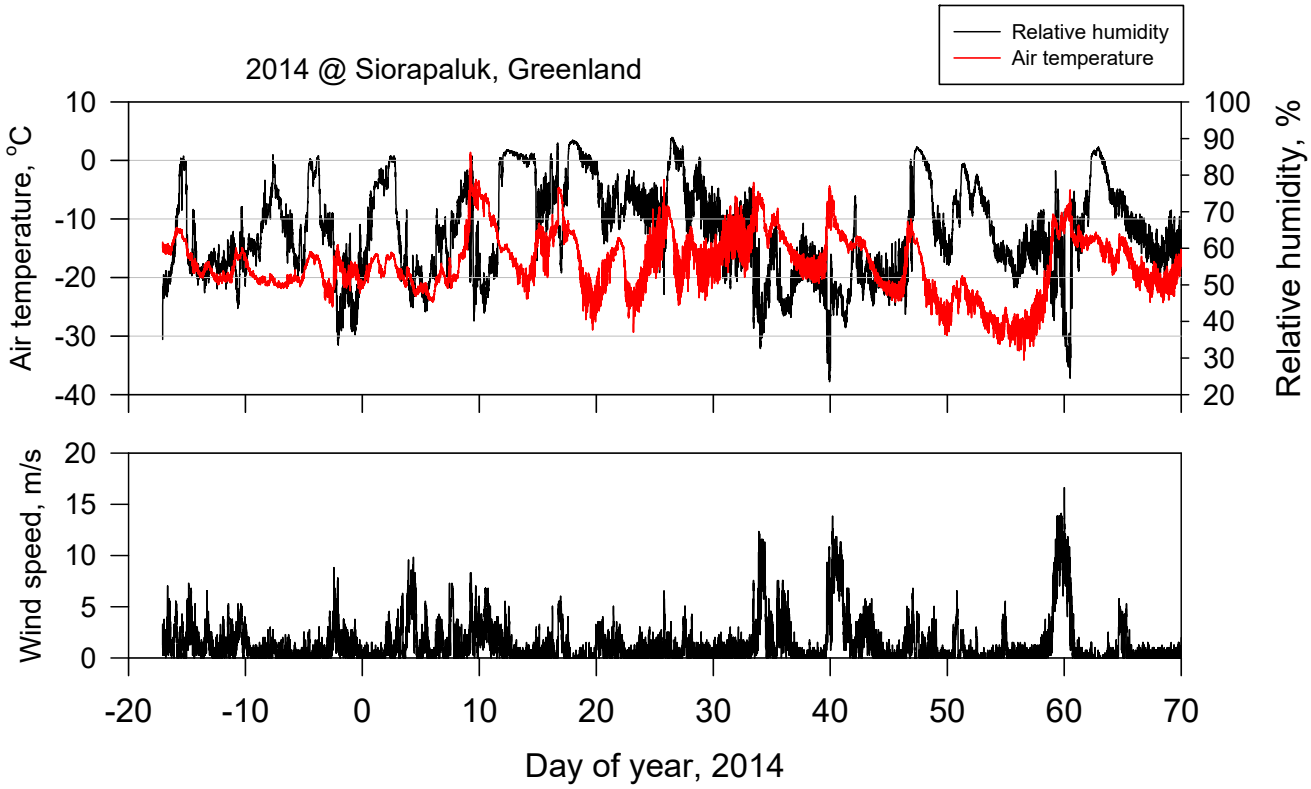

Figure 2 Variation of air temperature, relative humidity, and wind speed at Siorapaluk.

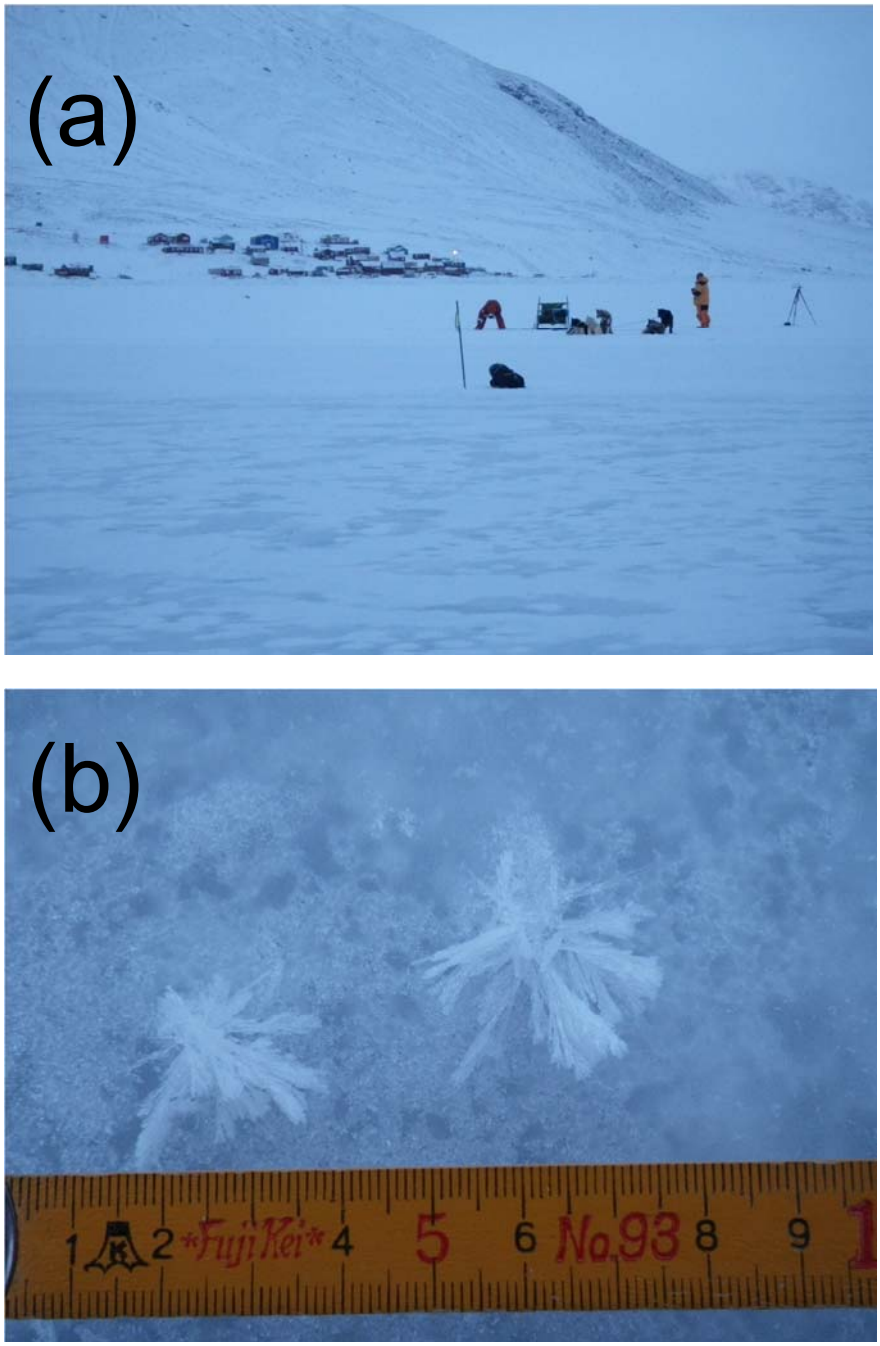

Fig.3

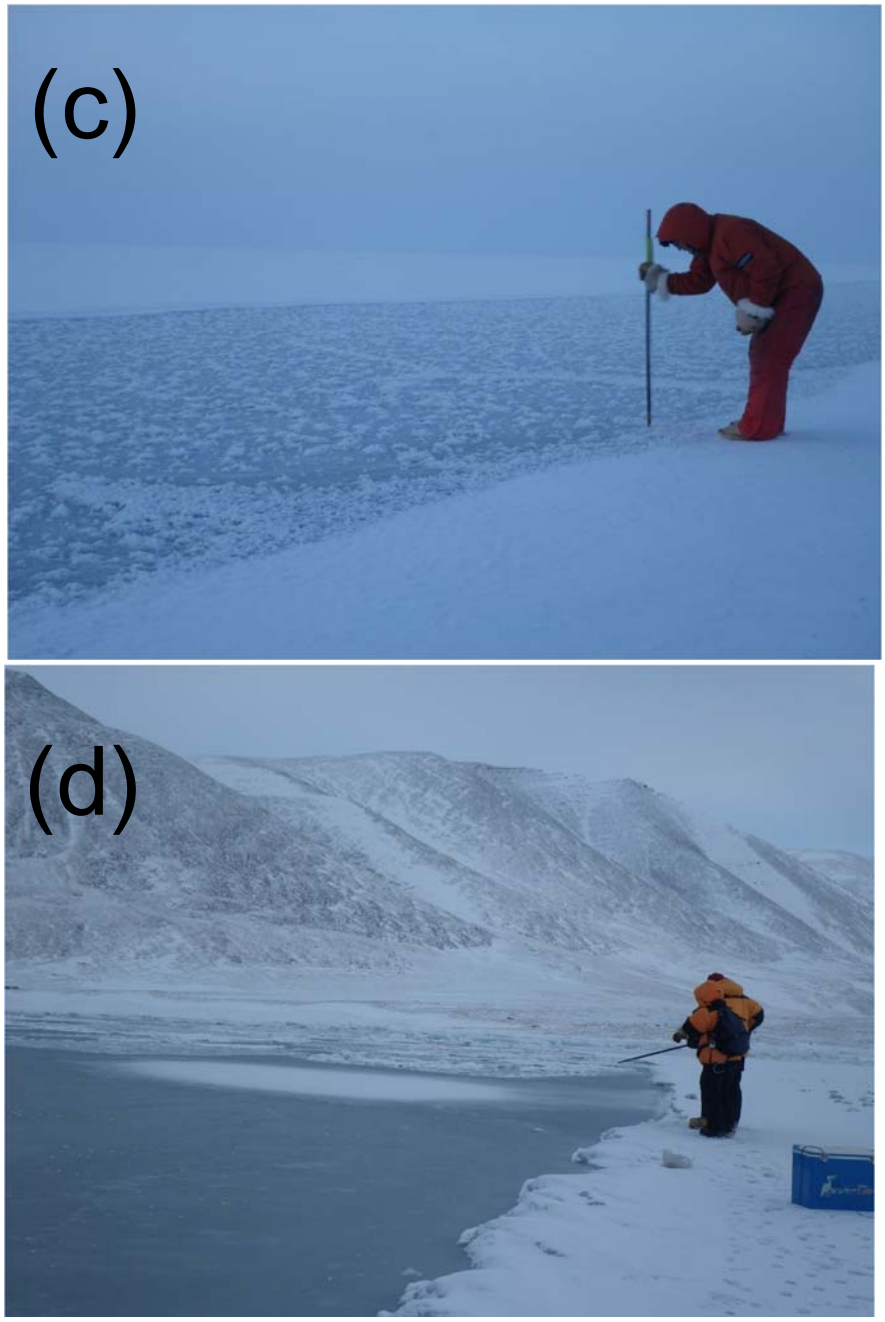

Fig.3

5

Figure 3 Photographs of (a) condition of sea-ice and frost flowers on 20 February at Site I , (b) frost flowers at Site I on 22 February, (c) frost flowers at Site II, (d) sea-ice condition at Site IIIa, (e) frost flowers on 4 March at Site IIIa, and (f) condition of old sea-ice on 2 March immediately after the storm.

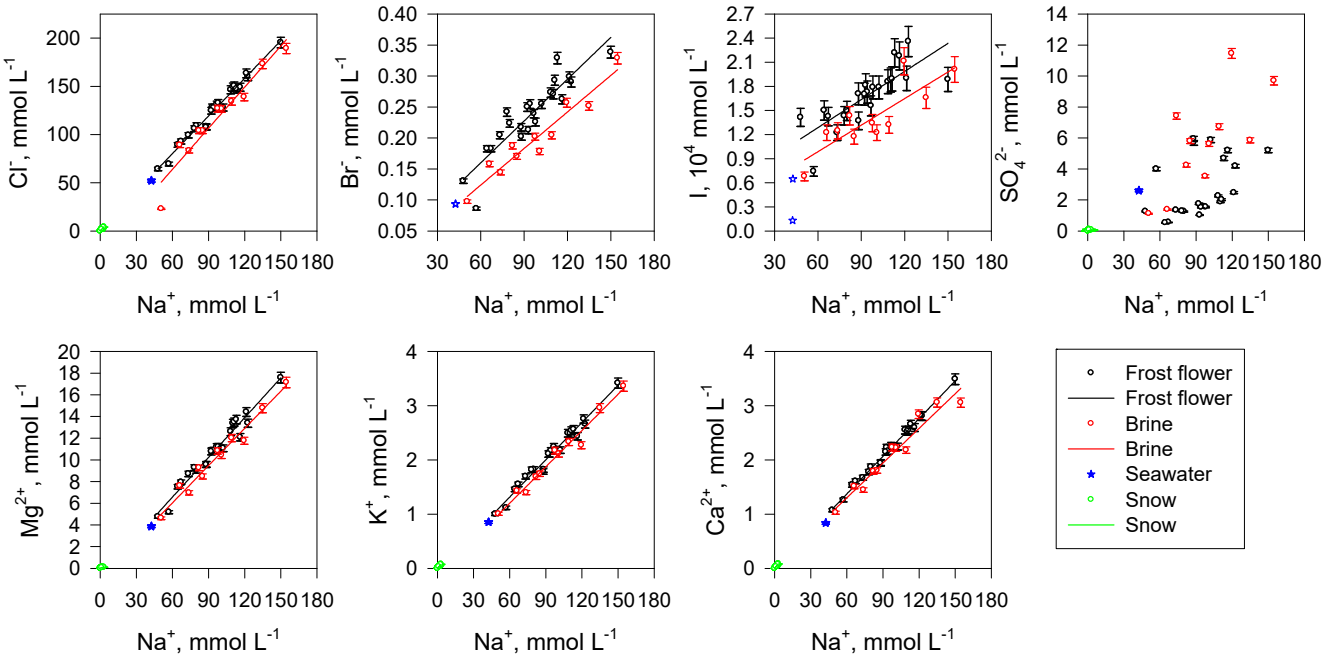

Figure 4 Relation among each constituent to Na^+ concentration of frost flowers, brine, and seawater taken in this study. Black and red lines respectively present regression lines of frost flowers and brine. Open black and red circles respectively present concentrations in frost flowers and brine. Filled blue stars represent the concentrations of seawater taken around Siorapaluk. Open blue stars represent the concentrations of seawater in the literature presented in Table 1. Error bars indicate analytical errors.

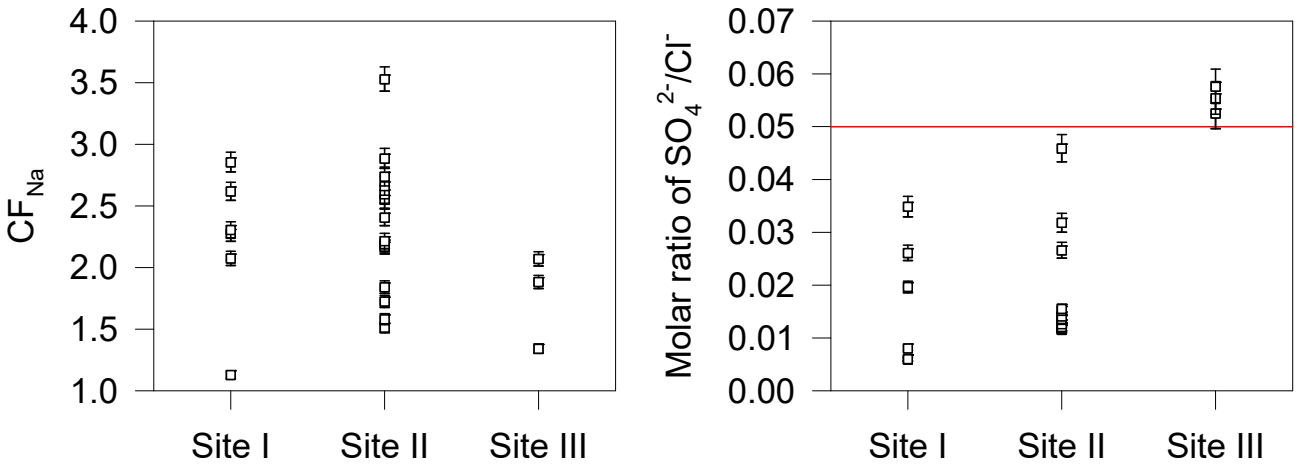

Figure 5 Variations of (a) concentration factor of Na^+ (CF_{Na}) and (b) molar ratios of SO_4^{2-}/Na^+ in frost flowers at each sampling site. Red line indicates the bulk seawater ratio. Error bars indicate analytical errors.

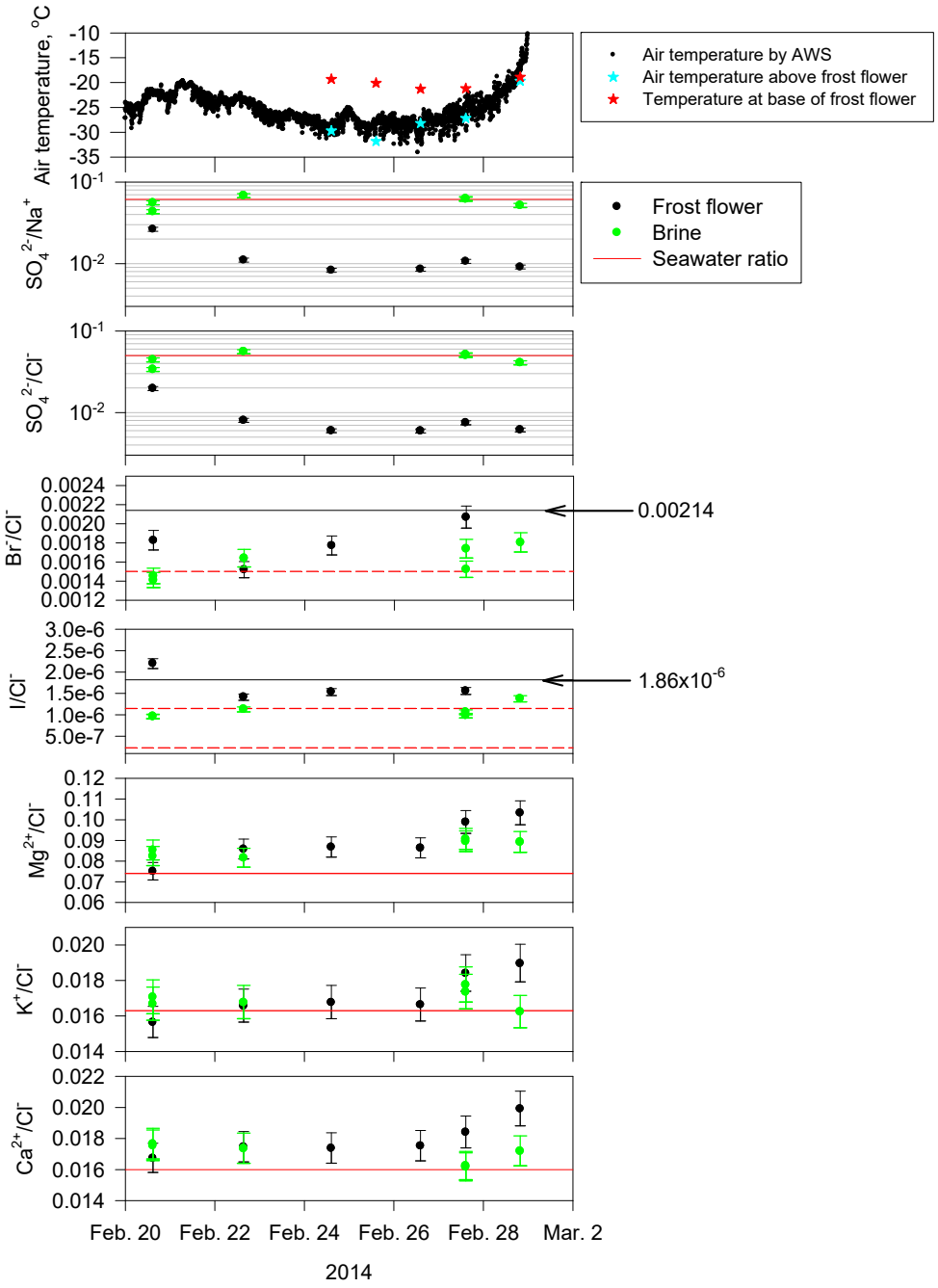

Figure 6 Short-term features of (a) air temperature measured by AWS (T_{AWS}), air temperature above frost flowers (T_{air}, ca. 10 cm above the sea-ice surface), temperature of base of frost flowers (T_{FF}), and (b–h) molar ratios of sea-salts in frost flowers and brine at Site I. T_{air} and T_{FF} were not measured on 20–22 February. Error bars indicate analytical errors. Black lines in Br-/Cl- and I/Cl- are the estimated ratios when hydrohalite precipitation occurs (Details are noted in section 4-2).

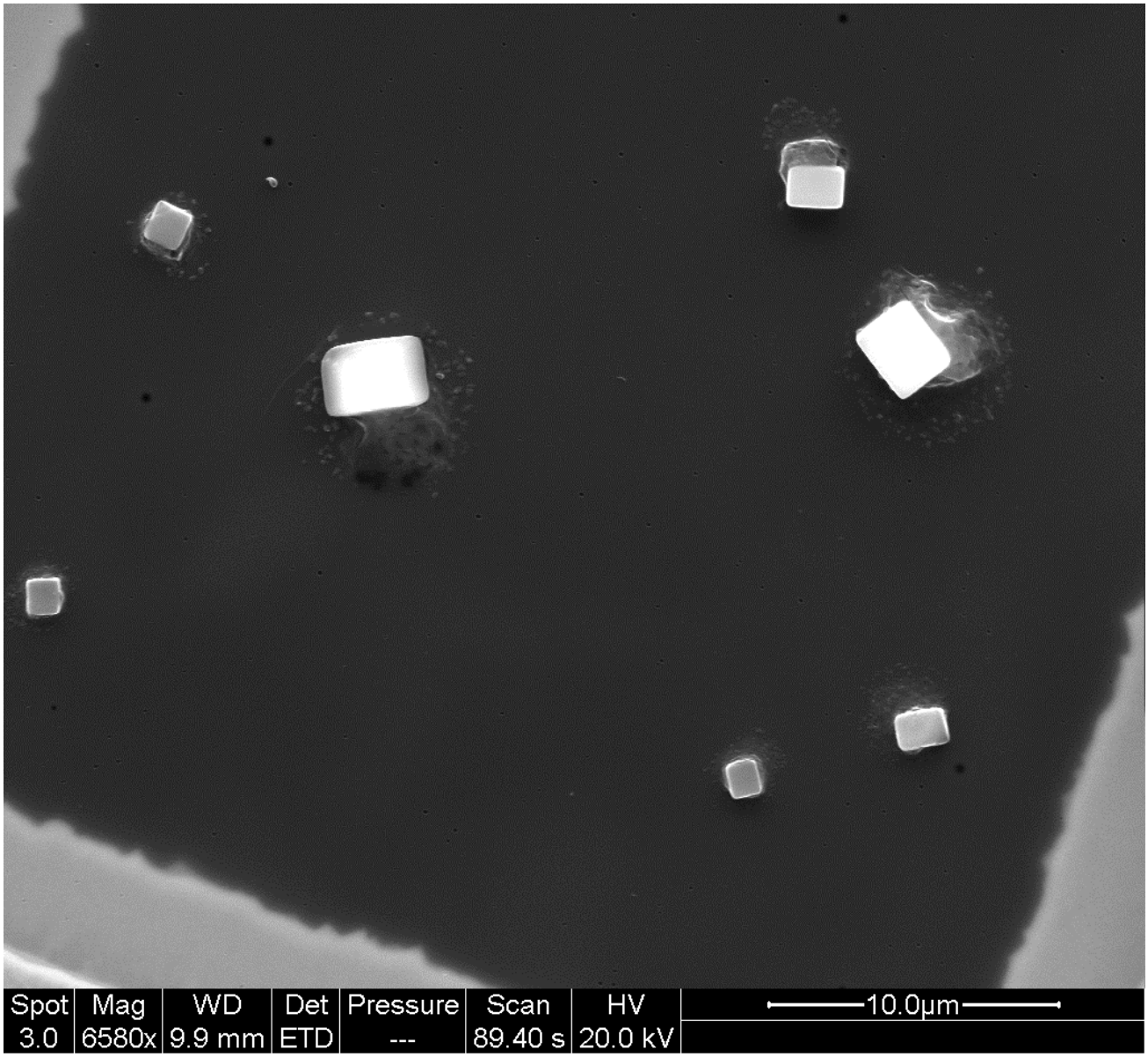

Figure 7 SEM image of aerosol particles collected on 1 March, 2014 above the sea-ice area with frost flowers.

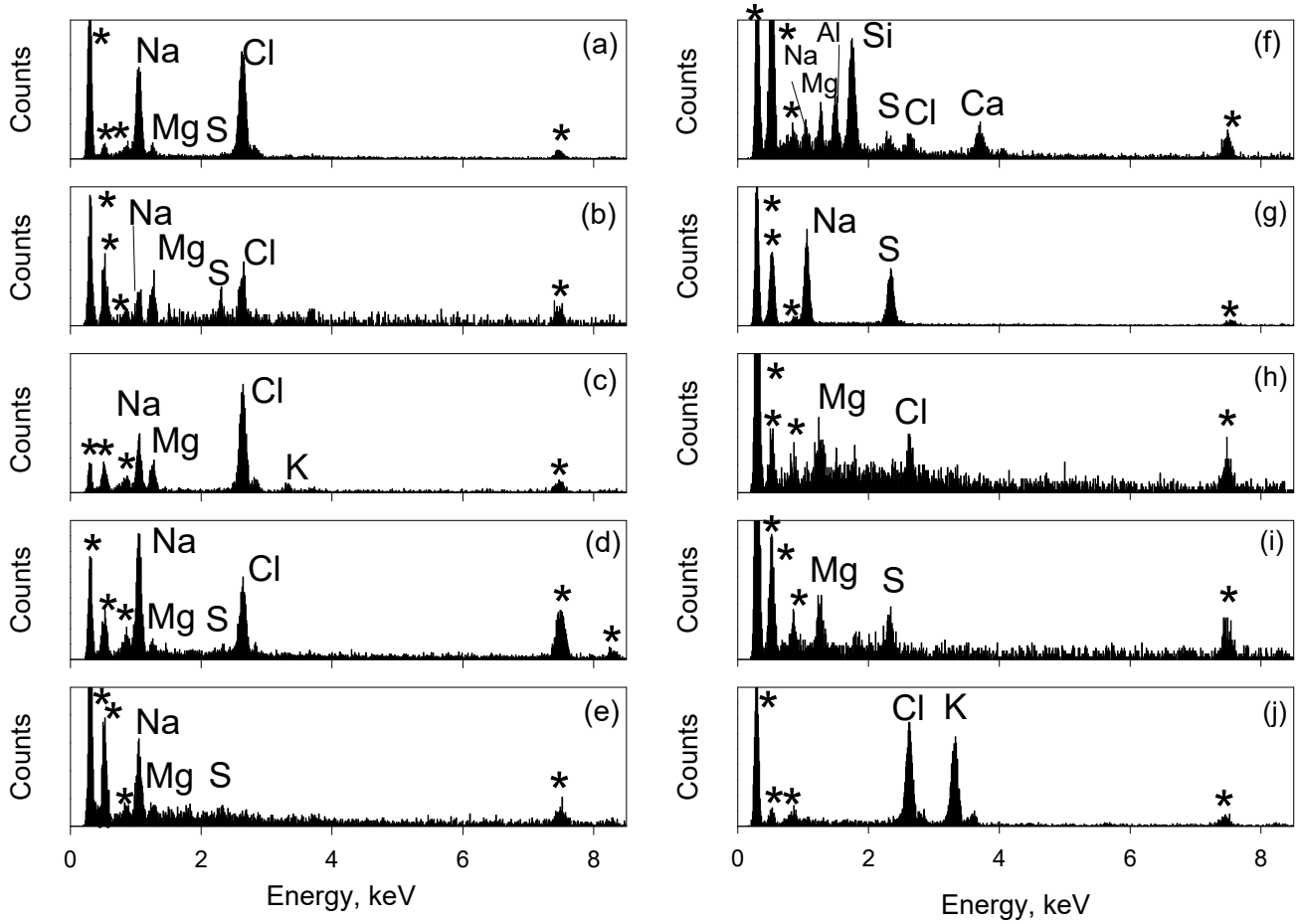

Figure 8 EDX spectra of sea-salt particles and sea-salt relating particles collected over the sea-ice area.

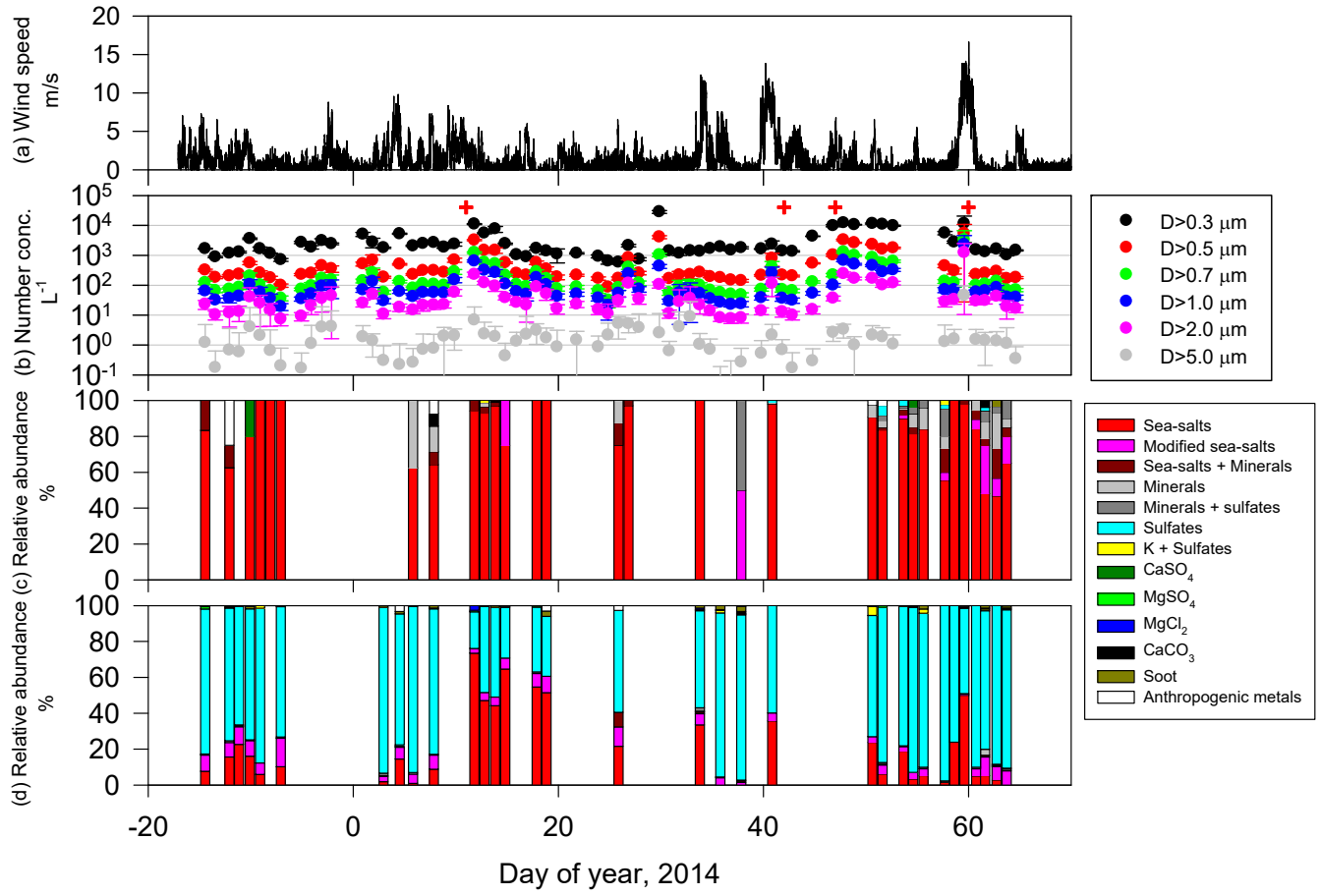

Figure 9 Variations of (a) wind speed, (b) aerosol number concentrations, relative abundance of each aerosol type in (c) coarse mode and (d) fine mode. Red + marks indicate the date when the low clouds (fogs) were identified off Siorapaluk.

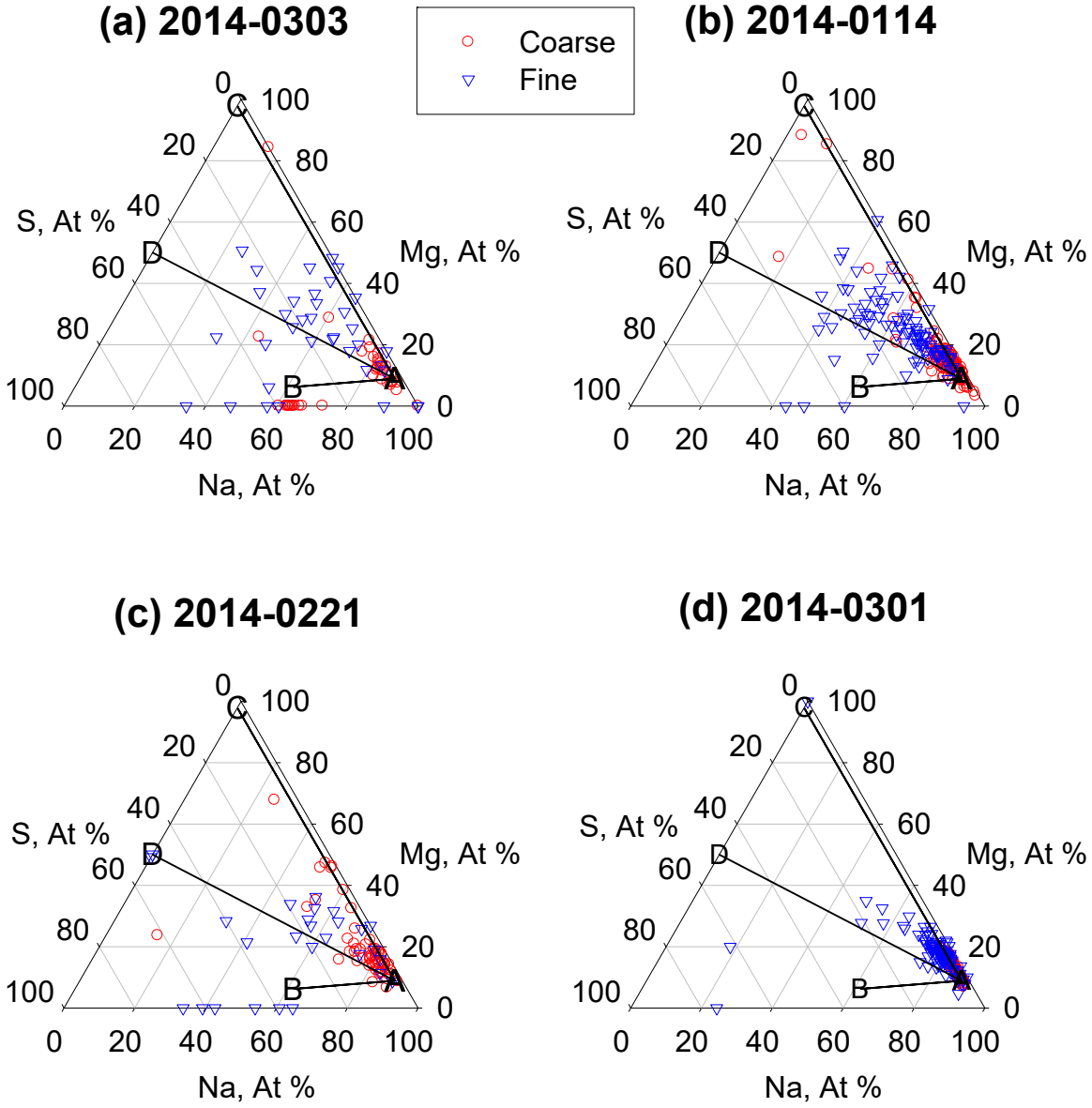

Figure 10 Ternary plots of Na–Mg–S of sea-salt particles and the modified sea-salt particles collected over the sea-ice area. A, B, C, and D in this figure denote respectively ratios of seawater, fully modified with SO_4^{2-}, $MgCl_2$, and $MgSO_4$,. Red open circles and blue triangles respectively present ratios of particles in coarse and fine modes.

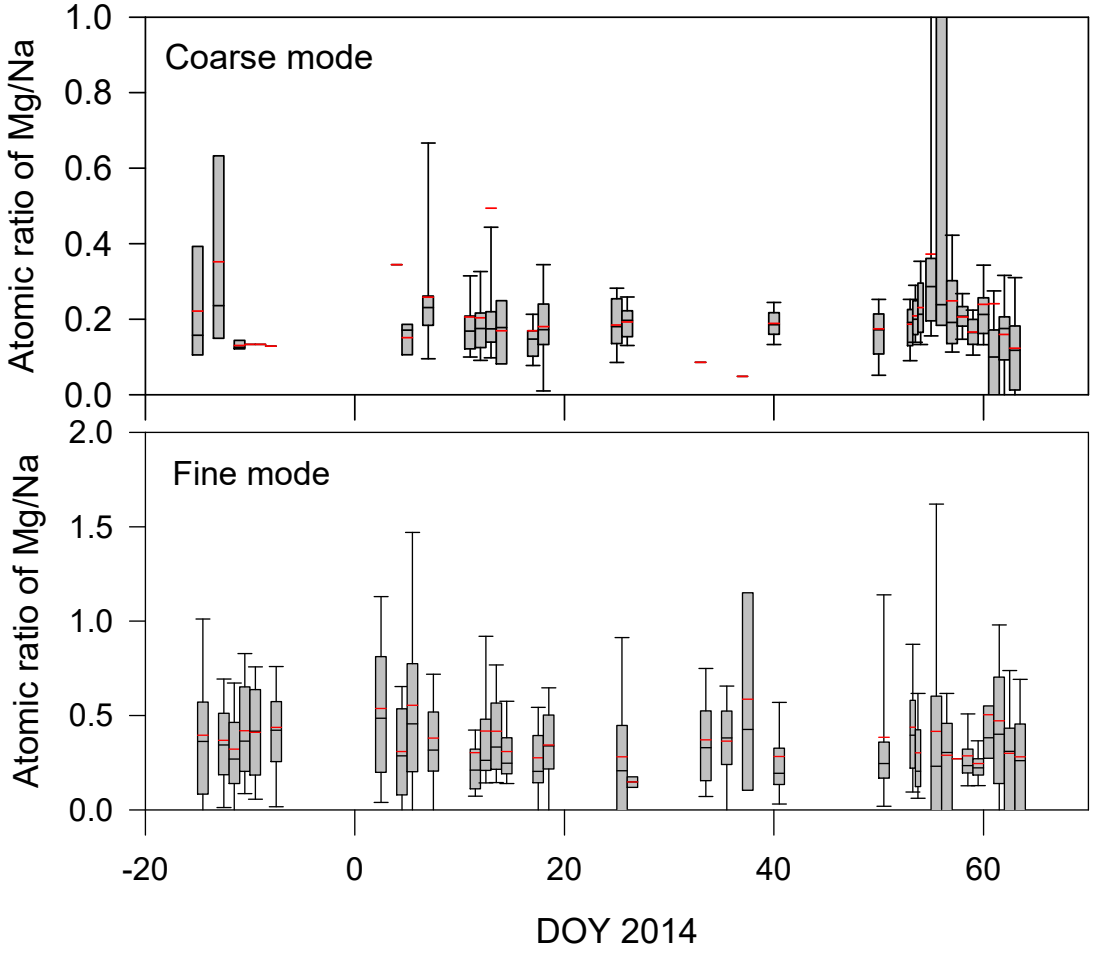

Figure 11 Variations of atomic ratios of Mg/Na in sea-salt particles and the modified sea-salt particles collected over the sea-ice area. In box plots, the top bar, top box line, black middle box line, bottom box line, and bottom bar respectively denote values of 90, 75, 50 (median), 25, and 10%. The red line shows mean values.

5

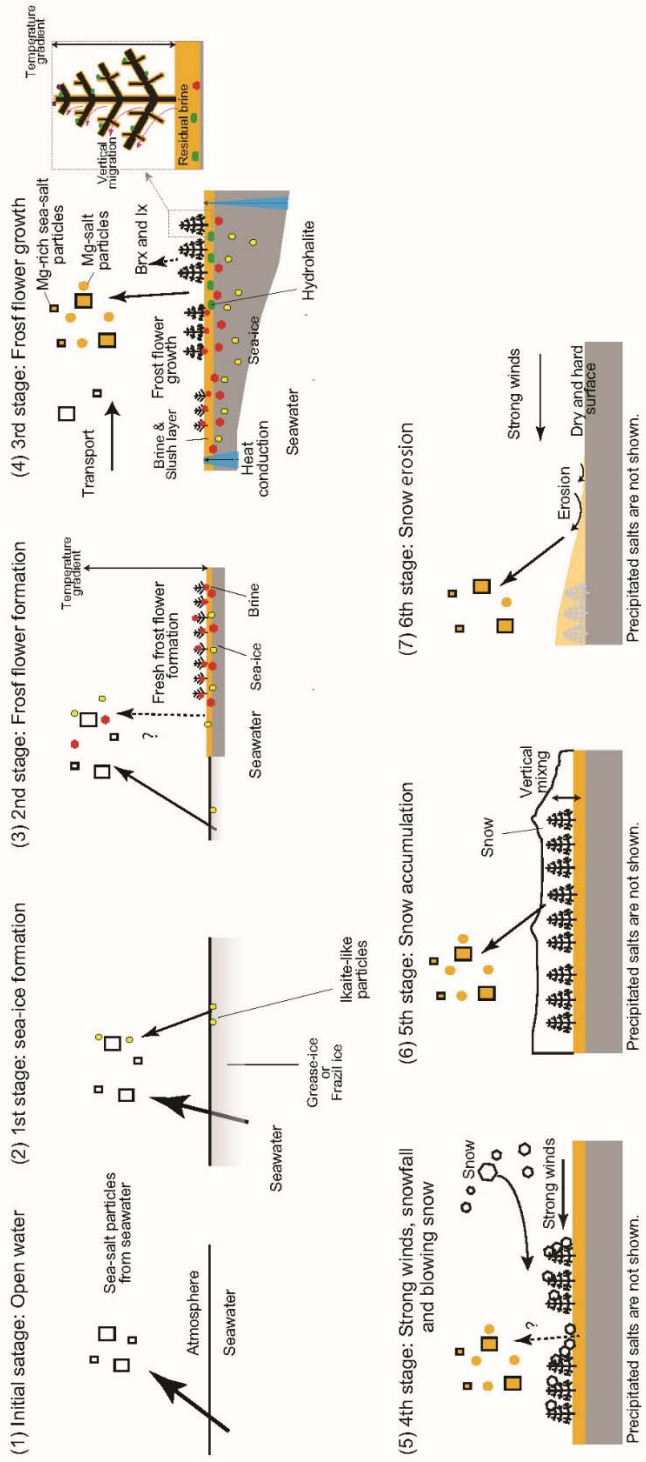

Figure 12 Schematics of sea-salt cycles in sea-ice area.

Table 1 Statics of molar ratios of sea-salts relative to Na^+ and Cl^- concentrations in frost flower, brine and seawater collected in this study ("n" indicates sample number).

		K^+/Na^+	Mg^{2+}/Na^+	Ca^{2+}/Na^+	Cl^-/Na^+	SO_4^{2-}/Na^+	Br^-/Na^+	I/Na^+	K^+/Cl	Mg^{2+}/Cl	Ca^{2+}/Cl	SO_4^{2-}/Cl^-	Br^-/Cl^-	I/Cl^-
Frost flower n=23	Ave	0.022	0.113	0.023	1.326	0.029	0.0025	1.83×10^{-6}	0.017	0.086	0.017	0.022	0.0019	1.38×10^{-6}
	STD	0.001	0.008	0.001	0.052	0.020	0.0003	3.38×10^{-7}	0.000	0.004	0.000	0.016	0.0002	2.42×10^{-7}
	median	0.023	0.116	0.023	1.351	0.019	0.0025	1.83×10^{-6}	0.017	0.086	0.017	0.014	0.0019	1.35×10^{-6}
	min	0.020	0.091	0.022	1.217	0.008	0.0015	1.26×10^{-6}	0.016	0.074	0.017	0.006	0.0012	9.65×10^{-7}
	max	0.023	0.121	0.024	1.387	0.070	0.0031	2.95×10^{-6}	0.017	0.093	0.018	0.058	0.0023	2.20×10^{-6}
Brine n=11	Ave	0.021	0.105	0.022	1.170	0.056	0.0020	1.46×10^{-6}	0.019	0.096	0.020	0.049	0.0019	1.35×10^{-6}
	STD	0.001	0.008	0.001	0.246	0.026	0.0002	2.47×10^{-7}	0.008	0.035	0.008	0.022	0.0008	5.77×10^{-7}
	median	0.021	0.109	0.022	1.230	0.056	0.0020	1.37×10^{-6}	0.017	0.085	0.017	0.049	0.0017	1.13×10^{-6}
	min	0.019	0.091	0.020	0.451	0.021	0.0018	1.21×10^{-6}	0.016	0.081	0.016	0.016	0.0014	9.56×10^{-7}
	max	0.022	0.115	0.024	1.346	0.101	0.0024	1.85×10^{-6}	0.044	0.202	0.045	0.089	0.0043	2.97×10^{-6}
Snow n=15	Ave	0.023	0.076	0.026	1.321	0.037			0.018	0.058	0.020	0.030		
	STD	0.001	0.030	0.002	0.188	0.029			0.002	0.024	0.002	0.026		
	median	0.024	0.070	0.026	1.303	0.025			0.018	0.054	0.020	0.019		
	min	0.020	0.032	0.021	1.065	0.010			0.012	0.024	0.014	0.007		
	max	0.027	0.122	0.029	1.953	0.108			0.020	0.095	0.022	0.101		
Seawater n=2		0.020	0.091	0.020	1.227	0.0613	0.0018 a)	2.76×10^{-7} ~ 1.37×10^{-6} b)	0.016	0.074	0.016	0.0500	0.0015 a)	2.32×10^{-7} ~ 1.15×10^{-6} b)

a) Molar ratios of Br^- were listed using bulk seawater ratio (Lide, 2005).

b) Iodine ($I^- + IO_3^-$) concentration in seawater was estimated from the concentrations of I^- and IO_3^- measured by Ito (1997, 1999), Hirooka et al., (2003), Ito et al. (2003), Chen et al. (2007), and Horikawa et al. (2016). The estimated iodine concentrations in seawater are 0.130 - 0.647 μmol L^{-1}. Upper and lower molar ratios of I/Na and I/Cl were calculated using the estimated iodine concentrations and the concentrations of N^+ and Cl^- by Lide (2005).